frontiers | Frontiers in Materials

TYPE Original Research
PUBLISHED 20 August 2024
DOI 10.3389/fmats.2024.1351554

OPEN ACCESS

EDITED BY
Luciano Feo,
University of Salerno, Italy

REVIEWED BY
Ionut Ovidiu Toma,
Gheorghe Asachi Technical University of Iași, Romania
Francesco Ascione,
University of Salerno, Italy

*CORRESPONDENCE
Alireza Bahrami,
alireza.bahrami@hig.se
Khalid Ansari,
ksansari@ycce.edu
Yasin Onuralp Özkılıç,
yozkilic@erbakan.edu.tr

RECEIVED 06 December 2023
ACCEPTED 09 April 2024
PUBLISHED 20 August 2024

CITATION
Wagh M, Waghe U, Bahrami A, Ansari K, Özkılıç YO and Nikhade A (2024) Experimental investigation of mechanical and durability performances of self-compacting concrete blended with bagasse ash, metakaolin, and glass fiber.
Front. Mater. 11:1351554.
doi: 10.3389/fmats.2024.1351554

Experimental investigation of mechanical and durability performances of self-compacting concrete blended with bagasse ash, metakaolin, and glass fiber

Monali Wagh[1], Uday Waghe[1], Alireza Bahrami[2]*, Khalid Ansari[1]*, Yasin Onuralp Özkılıç[3,4]* and Anshul Nikhade[5]

[1]Department of Civil Engineering, Yeshwantrao Chavan College of Engineering, Nagpur, India, [2]Department of Building Engineering, Energy Systems and Sustainability Science, Faculty of Engineering and Sustainable Development, University of Gävle, Gävle, Sweden, [3]Department of Civil Engineering, Necmettin Erbakan University, Konya, Türkiye, [4]Department of Civil Engineering, Lebanese American University, Byblos, Lebanon, [5]Department of Civil Engineering, KDK College of Engineering, Nagpur, India

This study investigated the effects of using bagasse ash (BA) and metakaolin (MK) together as substitutes for cement in self-compacting concrete (SCC), together with the addition of glass fiber (GF), on the physical and mechanical characteristics of concrete. Eighteen SCC mixes were created, each containing different proportions of BA (0%, 10%, 15%, and 20%), MK (0%, 10%, 15%, and 20%), and BA and MK collectively (10% + 5% and 10% + 10%) as cement replacements with and without 0.1% GF. Using the results of the slump flow, T500 slump flow, V-funnel, and L-box tests, the performance of fresh SCC was determined. Furthermore, this study evaluated the strength, durability, and microstructural properties of the SCC samples. The SCC mix blended with 10% BA and 5% MK revealed better flowability as the slump flow increased from 692 mm to 715 mm. A strong linear correlation was discovered between the slump flow values (mm) and V-funnel duration (sec) and blocking ratio (H_2/H_1) with R^2 = 0.8876 and R^2 = 0.8467, respectively. Of all test mixes, the SCC mix blended with 10% BA, 5% MK, and 0.1% GF (SCC1B10M5) demonstrated the highest degree of strength. At 56 days, the 10% BA, 5% MK, and 0.1 GF mix had 12.8%, 25.7%, and 22.2% higher compressive, flexural, and splitting tensile strengths than the control mix, respectively. SCC, combined with BA, MK, and GF, outperformed the control mix. After immersion in a 3% H_2SO_4 solution, the SCC mix having 10% BA, 5% MK, and 0.1% GF experienced a minimum reduction in weight loss and ultrasonic pulse velocity of 1.01% and 3.1%, respectively. Additionally, there was a decrease of 29.4% in the percentage of charges passed. The ideal composition

Abbreviations: SCC, self-compacting concrete; BA, bagasse ash; MK, metakaolin; GF, glass fiber; VMA, viscosity-modifying admixture; CS, compressive strength; FS, flexural strength; STS, splitting tensile strength; UPV, ultrasonic pulse velocity; RCPT, rapid chloride penetration test; SEM, scanning electron microscopy; EDX, energy-dispersive X-ray; XRD, X-ray diffraction.

was achieved by incorporating 10% BA, 5% MK, and 0.1% GF into the SCC mixture, resulting in a dense structure without any visible pores or cracks during the microstructural analysis.

KEYWORDS

self-compacting concrete, bagasse ash, metakaolin, segregation, sustainability

1 Introduction

Since the early 1990s, when self-compacting concrete (SCC) first entered the construction sector, significant study and development efforts have focused on achieving and evaluating its rheological properties (Domone, 2007). Okamura and Ouchit (2018) first suggested the idea of SCC in 1986 and created the prototype in 1988. SCC is a distinctive concrete that can be poured and compacted by its weight without extra vibratory effort because of its exceptional deformability and cohesiveness (Shi et al., 2015; Patil et al., 2024). Concrete is the foundation of the current constructed environment (V Bekun et al., 2023; Alola et al., 2023; Iftikhar et al., 2023; Hajali et al., 2016; Fayed et al., 2023). Therefore, improvements in concrete technology have been increasing with various studies (Akhmetov et al., 2022; Wang et al., 2022; He et al., 2023; Yao et al., 2023; Zhou et al., 2023), and these have also led to an increase in the use of concrete. The imminent increase in global population and urbanization rates over the coming decades foreshadows concerning statistics regarding the environmental repercussions of this extensive use of concrete (Gerges et al., 2018; Scrivener et al., 2018; Antoun et al., 2021; Gerges et al., 2022; Saeed et al., 2022). Cement is a binding ingredient, which results in higher CO_2 emissions (Celik et al., 2023a; Aksoylu et al., 2023; Gerges et al., 2023). Developing a long-term, ecologically sensitive, and environmentally sustainable plan is necessary because of the mounting threat that global warming poses to human society (Issa and Salem, 2013; Gupta et al., 2021; Farrant et al., 2022; Celik et al., 2023b; Jahami and Issa, 2023). Due to technological advancements, rising standards of living, expanding urbanization, and an increasing population have increased the demand for natural resources in the building industry, leading to resource scarcity (Othuman Mydin et al., 2023; Ozkılıç et al., 2023; Tu et al., 2023; Waqas et al., 2023). Motivated by the lack of resources, researchers aimed to utilize solid waste produced by commercial, industrial, domestic, and farming operations as a replacement for raw materials for concrete (Agrawal et al., 2023; Zhang et al., 2023a; Zhang et al., 2023b; Chen et al., 2023; Bai et al., 2024). India has produced more than 600 tons of agricultural waste, which raises the issue of disposal. Reusing this residue as a supplementary cementitious material (SCM) eliminates waste scrapping problems and provides a low-cost construction material (Madurwar et al., 2013; Prusty et al., 2016; Meshram et al., 2023). The use of SCMs in construction contributes to the reduction in CO_2 (Abed et al., 2022). To reduce CO_2 pollution, concrete construction can use SCMs (Ahmad et al., 2021). Using waste in concrete helps protect against environmental threats (Agrawal et al., 2023; Tang et al., 2023; Pang et al., 2024). Figure 1 represents a cluster of network visualization using keywords from the research articles reviewed for this experiment.

Numerous studies have supported the utilization of agricultural wastes as an alternative cementitious pozzolanic material. Owing to their accessibility and pozzolanic properties, emphasis on this scrap has been suggested (Mannan and Ganapathy, 2004; Kumar Jagarapu and Eluru, 2020; Ahmad et al., 2021; Quedou et al., 2021). Pozzolanic substances favorably affect the rheology of the concrete mix, as well as its hardened strength and durability (Kumar Jagarapu and Eluru, 2020; Wagh and Waghe, 2022). The fiber-filled residue that remains after the sugarcane juice is called bagasse (Nikhade et al., 2023). Because of the auto-combustion process in the cogeneration boilers, sugarcane produces bagasse ash (BA), as shown in Figure 2. As a pozzolanic substance, sugarcane BA presents a promising alternative to cement as a binder in concrete production (Mostafa et al., 2022). Instead of some of the cement material, the cementitious material BA was used to decrease environmental contamination (Quedou et al., 2021). Compared with other oxides, the SiO_2 proportion in BA is more significant (EFNARC, 2002; Sua-Iam and Makul, 2013; Setayesh Gar et al., 2017; Le et al., 2018; Waghe et al., 2023). The outcomes of SCC were improved when BA was utilized as a partial cement substitution (Das et al., 2022). The environmentally benign use of rice husk ash (RHA) and BA-mixed ashes enhanced the physical and mechanical characteristics and sulfate protection of SCC (Hamza Hasnain et al., 2021). Wagh and Waghe (2023) assessed the rheological characteristics of SCC with BA, metakaolin (MK), and glass fiber (GF). A more cost-effective and environmentally friendly option is to use BA in SCC (Mim et al., 2023). In India, approximately 10.0 million tons of BA are processed as surplus, and the global sugarcane output is more than 1.5 billion tons (Prusty et al., 2016). Compared with control concrete, the cost of SCC, including 15% BA, is 35.63% lower (Akram et al., 2009).

Heating China clay between 600°C and 800°C produces MK as a by-product (Seelapureddy et al., 2021). MK provides better workability and requires less water-reducing admixture to achieve fresh properties, and its particles are notably smaller than cement particles (Ding, 2002; Hassan et al., 2012). Better workability may be attributed to the rounded and smoother particles of MK. The overall mechanical and durability qualities are improved because of the reaction of MK with calcium hydroxide during the hydration process (Hassan et al., 2012). MK enhanced the early mechanical and long-term strength properties (Siddique and Klaus, 2009). MK was used as a partial replacement for cement in the mixes, which positively impacts the freshly mixed and cured properties. The calcium silicate hydrate (C-S-H) gel and crystal formation were produced through the pozzolanic process (Asteris et al., 2022). With the application of MK, a substantial improvement in the pore structure and a decrease in $Ca(OH)_2$ in concrete have been noted. This is a result of the strong pozzolanic reactivity and purity of the cement. The microstructure of concrete was improved by the reaction of MK with $Ca(OH)_2$

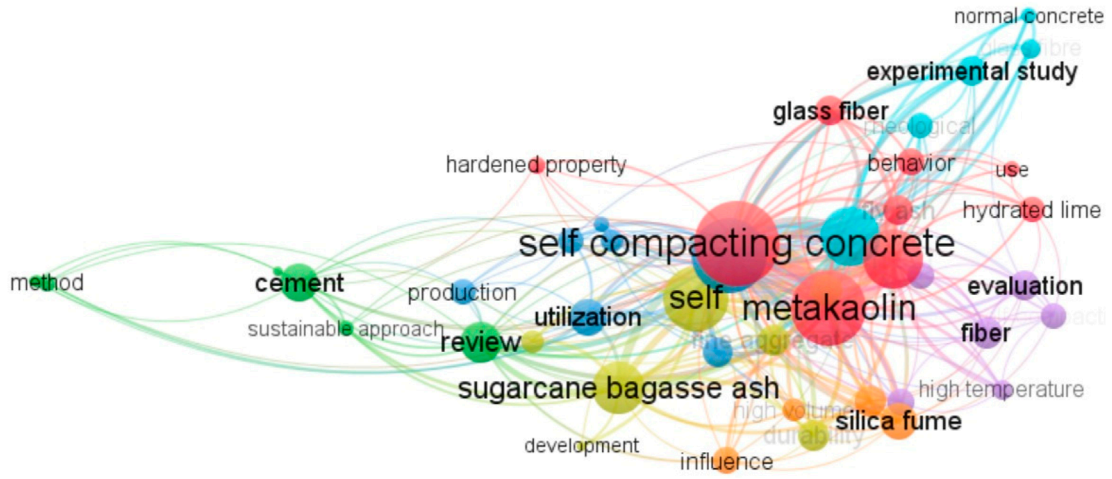

FIGURE 1
Network visualization of a cluster created using keywords of research articles from 2018 to 2023.

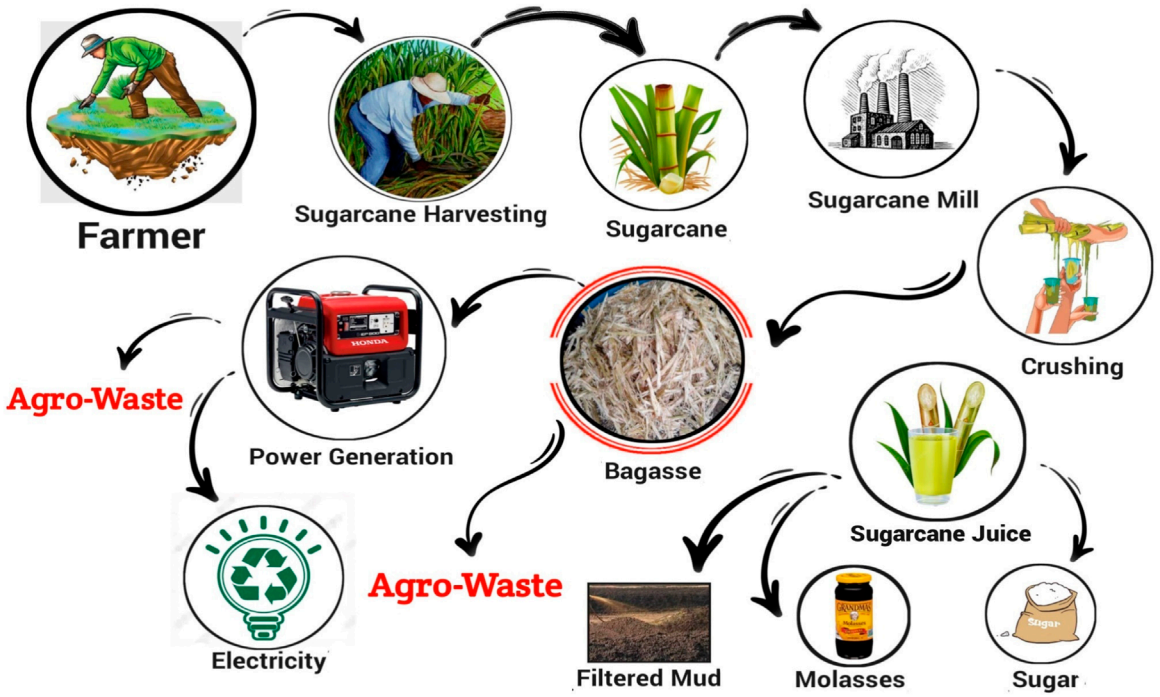

FIGURE 2
Schematic view of agro-waste BA.

to create an extra C-S-H gel, which enhanced the mechanical and durability qualities of the material (Danish and Mohan Ganesh, 2021). MK typically comprises 40%–45% Al_2O_3 and 50%–55% SiO_2. There are also a few trace amounts of Fe_2O_3, TiO_2, CaO, and MgO particles. In order of magnitude, MK particles are typically finer than cement particles (Bureau of Indian Standards BIS, 2000; Poon et al., 2001). A considerable improvement in the defense against chloride penetration is demonstrated in concrete containing MK (Nikhade and Pammar, 2022). The strength and durability of concrete were considerably increased by replacing 30% of cement with BA, MK, and RHA (Nikhade and Nag, 2022). Outstanding mechanical strength was achieved in geopolymer composites because of the pozzolanic activity and amorphous structure of ultrafine fly ash (Li et al., 2023).

The influence of GF on the initial and hardened characteristics of SCC was evaluated by Ahmad et al. (2017). After fibers were incorporated into concrete, the slump and slump flow diameter gradually decreased (Sanjeev and Sai Nitesh, 2020). GFs contributed toward improving the compressive strength (CS). Surface hardness increased with fibers, and uniformity was outstanding and decreased

FIGURE 3
Raw materials for SCC: **(A)** raw BA, **(B)** sieved BA, **(C)** MK, and **(D)** GF.

with greater fiber volume (Sivakumar et al., 2017; Mahakavi et al., 2021). Higher splitting tensile strength (STS) and flexural strength (FS) were determined in SCC composites supplemented with GF and polyvinyl alcohol (PVA) fiber up to a fiber dosage of 0.3% (Ahmad and Umar, 2018). Mechanical performance was enhanced by fibers (Lin et al., 2023). FS was improved by 10.5% by adding GF to SCC (Akhmetov et al., 2022). The findings indicated that the lowest rate of workability enhancement was observed in SCC with 2% and 4% nanosilica substitutions and the highest amount of GF (Bureau of Indian Standards BIS, 2021). The findings illustrated that the STS and FS of hybrid fiber-reinforced concrete were remarkably influenced by the fibers (Huang et al., 2021). The corrosion resistance performance of fiber-reinforced polymer bars is superior (Sun et al., 2023).

Several experiments have been performed on SCC using fly ash, BA, MK, steel fibers, polypropylene fibers, etc. However, only a few experiments were performed using BA in SCC along with MK and GF. Very few researchers concentrate on microstructural analysis and acidic effects on SCC.

The principal objective of this study was to use MK and BA as SCCs and GF to enhance the strength properties because it has been noted in the literature that SCC mixed with BA, MK, and GF performs better in terms of strength and durability.

Therefore, the purpose of this research was to determine the ideal ratio of cement replacement by BA and MK. To that end, BA and MK were utilized alone (0%–20%) and along with a proportion of BA (0% and 10%) and MK (0%, 5%, and 10%) combined with GF (0% and 0.1%). In terms of freshness and strength characteristics, the optimal mix of SCC with BA, MK, and GF was determined. The resistance of the produced SCC mixes to sulfuric acid assault both with and without BA, MK, and GF was assessed. The current research aimed to understand how normal and acidic environments affect the development of SCC to meet the durability parameters. The microstructural analysis was conducted on SCC blended with BA, MK, and GF to investigate the mechanism underlying the sulfate attack-induced degradation of the SCC specimens.

2 Materials and methods

BA was procured from a sugarcane mill in Devhala, Tumasr, India. MK and GF were purchased from Apple Chemie Pvt. Ltd (Nagpur). From locally accessible construction supplies, coarse and fine aggregates were extracted. To develop SCC, grade 43 ordinary Portland cement was used, following IS 8112 (Bureau of Indian Standards BIS, 2013). Cement has a specific gravity of 3.15. Fine and coarse aggregates utilized in the studies met the requirements of IS 383 (Bureau of Indian Standards BIS, 2016). The sizes of coarse aggregates were 10 mm and 20 mm, whereas a 4.75-mm sieve was utilized to sift the fine material. Coarse aggregates of 10 mm and 20 mm with specific gravity values of 2.86 and 2.90 were used per the IS requirement, respectively. The specific gravity of fine aggregate was 2.68. ViscoFlux 5507 was utilized in SCC as a superplasticizer to reduce the water requirement. At 27°C and pH of more than 6, the relative density was 1.11. This product was certified using ASTM C494 types A and F and IS 9103-1999. The viscosity-modifying admixture (VMA) in SCC was AC-Gel-Build.

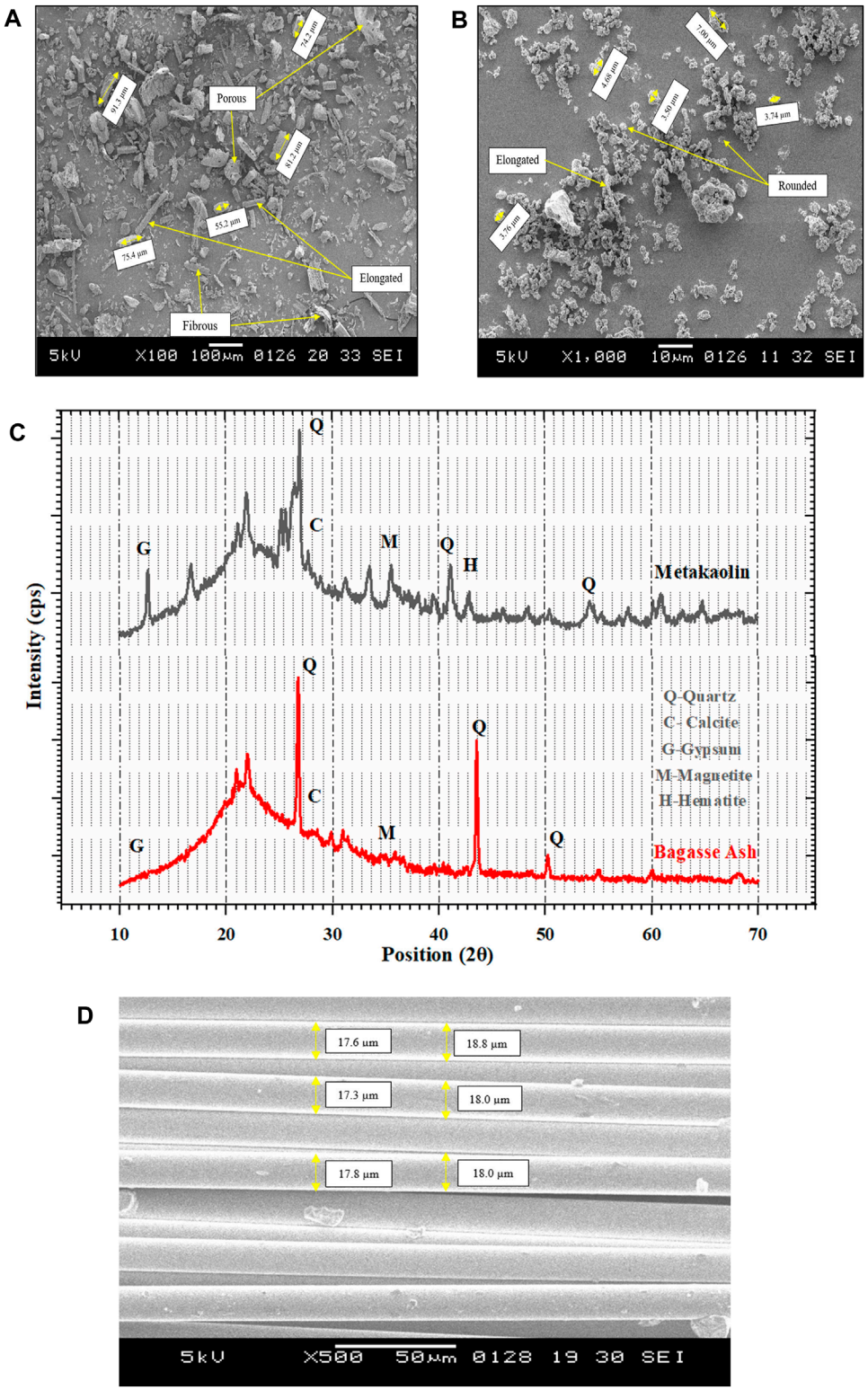

FIGURE 4
SEM images of: **(A)** BA and **(B)** MK, **(C)** XRD image of MK and BA, and **(D)** SEM image of GF.

The pH value varied from 5 to 8, and the density ratio was 1. This product was validated using IS 9103-1999. Supplementary Figure S1 shows the flowchart for the work process of this study.

After procurement, BA was dried and heated at 500°C for 1 day and then sieved using a 90-µ sieve. XRF testing of MK and BA was conducted at IBM, Nagpur. Supplementary Table S1

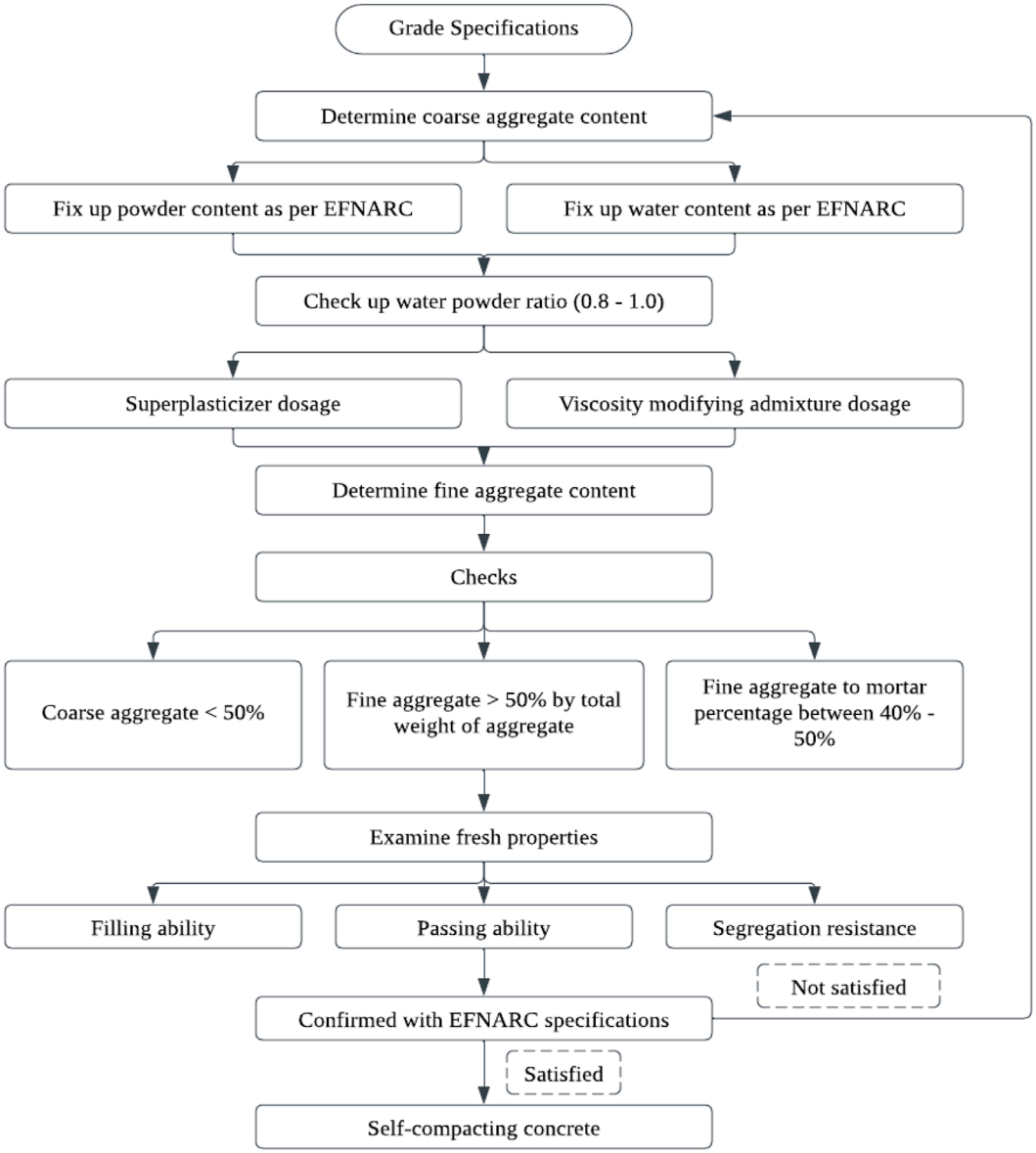

FIGURE 5
Mix design of SCC.

presents the chemical compositions of MK, BA, and cement. MK contributes significantly as a source of aluminum and silica in the composition, as noted by the larger percentages of Al_2O_3 (37.1%) and SiO_2 (54.9%) in this material. BA may be a considerable source of silica in the combination because of its high SiO_2 concentration (74.4%) compared with the other ingredients. Figure 3 displays the raw materials utilized in the study. Figures 3A, B show the gray color of BA, which has a specific gravity of 1.9. Most studies concur that treating BA is preferable to increasing its pozzolanic property (Amin et al., 2022). MK is a powder with an off-white shade, as shown in Figure 3C. Regarding size, 50% of the particles were below 1.72 μ. It was observed that MK had a specific gravity of 2.6. Figure 3D shows a scattered GF with a length of 3 mm.

The particles of BA are smaller than those of cement, but MK particles are notably smaller than both BA and cement particles. Figure 4 shows scanning electron microscopy (SEM) and X-ray diffraction (XRD) images of BA, MK, and GF, which were used to characterize the micro- and nanoparticles of the materials. Figure 4A shows that the SEM results revealed that the shapes of BA particles are irregular, elongated, non-smooth, and porous. SEM of BA indicates characteristics like a trapezoidal shape and fibrous nature. Figure 4B shows that the shapes of some of the MK particles were rounded and angular with smooth surfaces of various sizes, and some of the particles were elongated. Most of the particle sizes of MK were between 3 μm and 7 μm. Figure 4C displays the results of the XRD examination of the sugarcane BA and MK samples used in this research. With quartz predominating, the sample showed peaks

10.3389/fmats.2024.1351554

TABLE 1 Mix proportions of developed SCC.

Mix	BA	MK	Aggregate		Cement	Water	Superplasticizer	VMA	GF
			Coarse	Fine					
	(kg/m^3)	(kg/m^3)	(kg/m^3)	(kg/m^3)	(kg/m^3)	(lit/m^3)	(%)	(%)	(%)
SCC	0	0	796.5	981.6	530	180	1.5	0.3	0
SCC1	0	0	796.5	980.3	530	180	1.6	0.3	0.1
SCCB10	53	0	796.6	951.8	477	180	1.5	0.3	0
SCCB15	79.5	0	796.6	936.9	450.5	180	1.5	0.3	0
SCCB20	106	0	796.6	922.1	424	180	1.5	0.3	0
SCC1B10	53	0	796.6	950.5	477	180	1.6	0.3	0.1
SCC1B15	79.5	0	796.6	935.6	450.5	180	1.6	0.3	0.1
SCC1B20	106	0	796.6	920.7	424	180	1.6	0.3	0.1
SCCM10	0	53	796.5	972.0	477	180	1.5	0.3	0
SCCM15	0	79.5	796.5	967.2	450.5	180	1.5	0.3	0
SCCM20	0	106	796.5	962.4	424	180	1.5	0.3	0
SCC1M10	0	53	796.5	970.7	477	180	1.6	0.3	0.1
SCC1M15	0	79.5	796.5	965.9	450.5	180	1.6	0.3	0.1
SCC1M20	0	106	796.5	961.1	424	180	1.6	0.3	0.1
SCCB10M5	53	26.5	796.6	941.8	450.5	180	1.9	0.3	0
SCCB10M10	53	53	796.6	937.0	424	180	1.9	0.3	0
SCC1B10M5	53	26.5	796.6	941.8	450.5	180	1.9	0.3	0.1
SCC1B10M10	53	53	796.6	937.0	424	180	1.9	0.3	0.1

mostly indicative of the following mineral phases: calcite, calcium phosphate, hematite, and mullite. Figure 4D depicts that the width of GF was between 16 μm and 18 μm. The cross-sectional form of the fibers was round in shape and had a smooth surface.

3 Experimental program

The SCC mix design was completed in compliance with the recommendations of EFNARC (2002). Figure 5 shows the design procedure as per the EFNARC guidelines. Based on the experience and recommendations, the starting mix proportions were estimated. These initial proportions served as a starting point for further changes during the mix design process. After various trials, a mix design was achieved, and fresh properties were within the range of the EFNARC guidelines. A total of 18 different SCC mixes were prepared, and Table 1 provides an in-depth look at the proportions of each mix. BA and MK were utilized as cementitious materials by adding 0%–20% to the weight of cement, respectively, to minimize the amount of ordinary Portland cement. The water content was kept constant at 180 lit/m^3. The water-to-powder ratio ranged from 0.85 to 1.1. Dosages for the superplasticizer ranged from 1.5% to 1.9%. The VMA was maintained at 0.3%.

3.1 Casting and testing

Following the EFNARC recommendations (EFNARC, 2002), fresh properties were used to evaluate the passing ability and flowability of the developed SCC. After all the concrete mixes were designed, specimens were cast for different tests and then left to cure for 28 days at room temperature in a curing tank accessible at the laboratory. In this research, the CS of concrete was analyzed using 150-mm cubes, and FS and STS were assessed using a 100 mm × 100 mm × 500 mm beam and a 150 mm diameter by 300-mm-long cylinders, respectively. All the mixtures that conformed to IS 516 and IS 5816 were utilized in this study. A compressive testing machine was used for obtaining the CS and STS. Two-point loading flexural

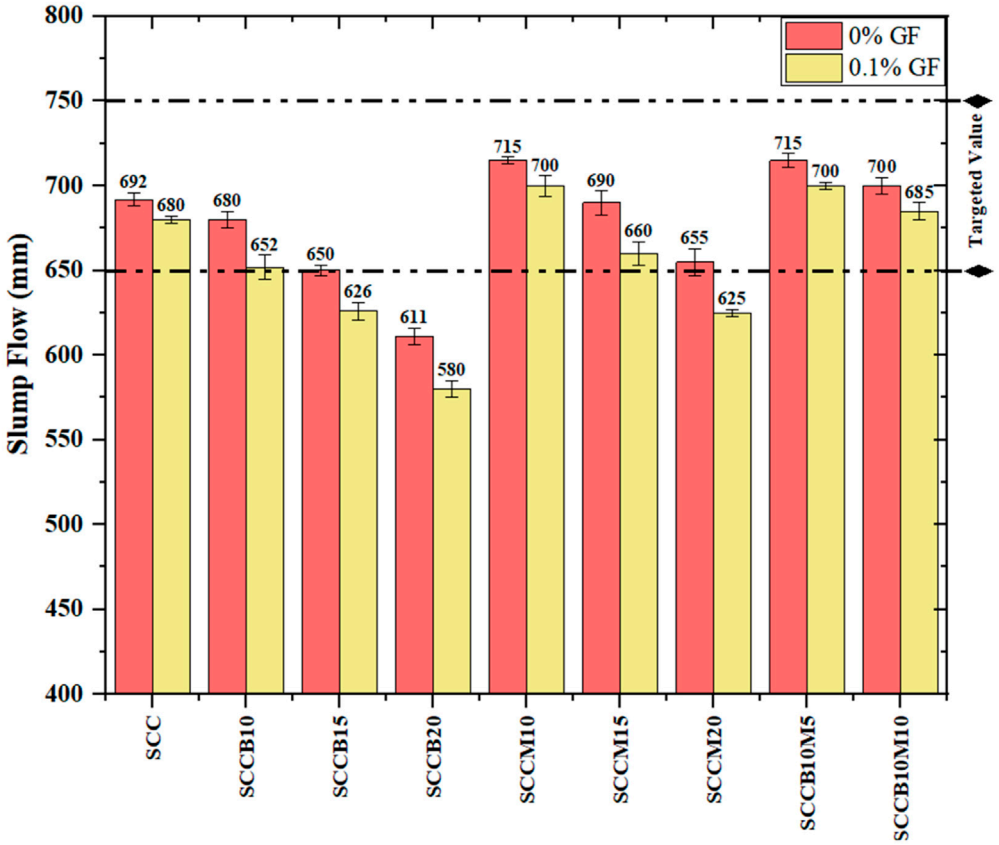

FIGURE 6
Comparison of slump flow for developed SCC.

testing equipment was used for obtaining FS, as per the Indian requirement. Ultrasonic pulse velocity (UPV) was also assessed using 150-mm cubes following the requirement of IS 13311. This nondestructive test indicated the uniformity and porosity of the samples. The two ultrasonic probes, as a transmitter and receiver, were positioned between the opposite edges of the specimens to determine the UPV using Equation 1.

$$\mathrm{UPV} = \frac{\mathrm{Length\,of\,specimen\,(m)}}{\mathrm{Travelled\,wave\,time\,(sec)}}. \quad (1)$$

A rapid chloride penetration test (RCPT) was also performed to examine the durability of the developed SCC samples using 100-mm diameter cylinders based on ASTMC1202 (ASTM, 2024). The experiment included measuring the amount of charge passed to the SCC specimens in a cell exposed to 60 V for 6 h on a 100-mm-diameter by 50-mm-depth concrete disk using Equation 2, where one of the electrodes was submerged in a solution of 3% sodium chloride (NaCl) and the other in a solution of 0.3% sodium hydroxide (NaOH).

$$Q = 900\left(Ic_0 + 2Ic_{30} + 2Ic_{60} + \ldots + 2Ic_{300} + 2Ic_{330} + Ic_{360}\right), \quad (2)$$

where Q is the passed charge in coulombs, Ic_o is the current in amperes just after the voltage is passed, and Ic_t is the current (amperes) at t minutes after the application of voltage.

Supplementary Figure S2 presents images of fresh properties obtained from the developed samples. The cast specimens and curing procedure are given in Supplementary Figure S3.

4 Results and discussion

The freshness, strength, and durability properties of all the developed SCC mixes are determined based on various requirements.

4.1 Fresh properties of SCC

4.1.1 Slump flow test

Slump findings for all the SCC combinations are displayed in Figure 6, with all the values falling within the specified limits of 550–750 mm for the slump flow based on EFNARC (2002). The slump flow measures the workability and flowability of concrete by showing how far it spreads when the slump cone is removed. The slump flow values varied in the SCC mixes containing various cement substitutes (such as BA and MK). The slump flow for the control SCC mixture was 692 mm without GF and 680 mm with 0.1% GF. The slump flow was marginally lowered by incorporating 0.1% GF, demonstrating a marginal effect on the workability and

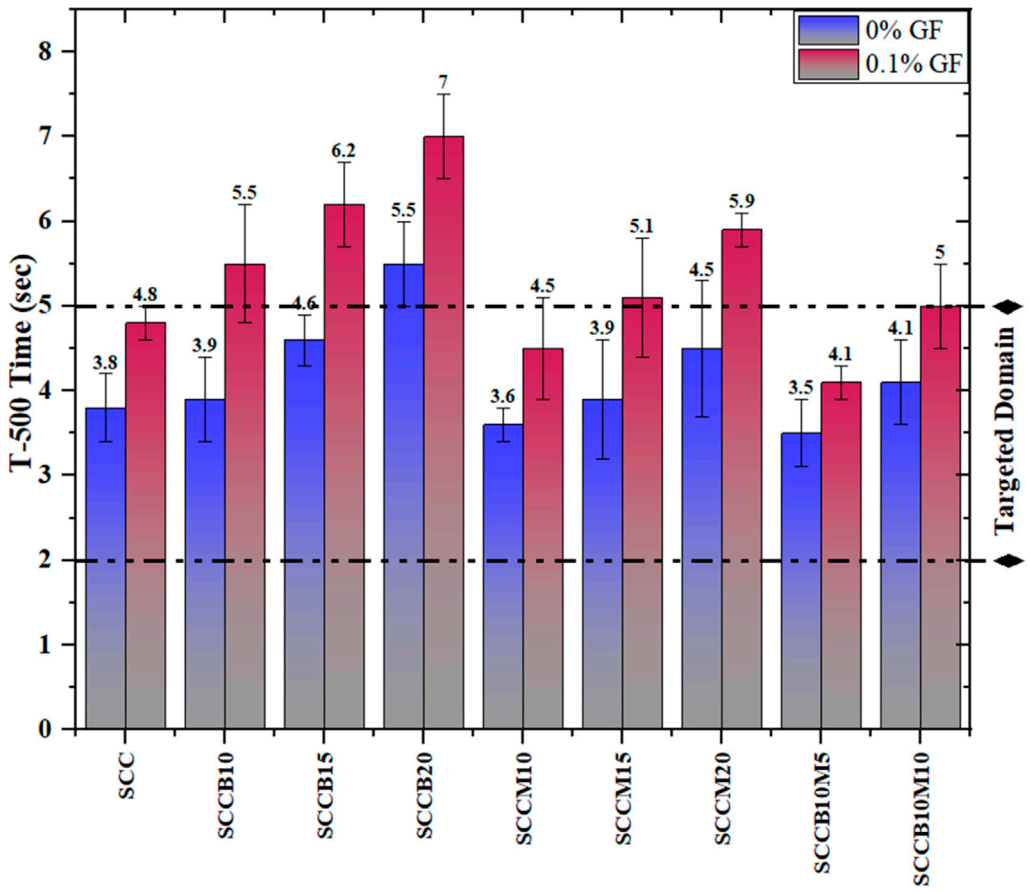

FIGURE 7
Variation in T500 slump flow time for developed SCC.

flow of concrete. The slump flow values typically decreased as the BA replacement percentage increased from 10% to 20%. This signified that the workability and flowability of SCC decreased with increasing amounts of BA. With a better slump flow rating than SCC, SCCM10 exhibited better workability and flowability. For SCCM10, the slump flow increased from 692 mm to 715 mm. This illustrated that replacing up to 10% of cement with MK in the concrete mix enhanced the flowability of the mixture. Again, increasing the proportion of MK in the SCC mixes also tended to result in a decrease in the slump flow values. The workability and flowability of SCC were enhanced by the use of the BA and MK substitutes, together with a slight increase in the dosage of superplasticizer. The SCCB10M5 mix had strong workability and flow, with the slump flow values of 715 (without GF) and 700 (with 0.1% GF). Due to its high slump flow, this mix had outstanding flow characteristics that enabled it to fill and flow through densely packed or complex reinforcement without vibration. The slump value test demonstrated that the slump value decreased with an increase in the proportion of GF in concrete (Tibebu et al., 2022). The appropriate degree of workability was maintained by a stronger integration of MK and BA (Larissa et al., 2020).

4.1.2 T500 slump flow test

Figure 7 depicts the T500 slump flow for all developed mixes. It exhibits concrete passing ability and viscosity. T500 readings marginally increased with 0.1% GF. As the percentage of BA replacement increased from 0% to 20%, the T500 values increased. This suggests that higher levels of BA replacement resulted in slower passing ability and concrete flow. The T500 time values for SCC with MK mixes were lower, up to 10% replacement. Reducing the T500 time for SCCB10M5 showed higher flowability and workability. The SCCB10M5 and SCCB10M10 mixes displayed variations in T500 values compared with the other mix configurations, as shown in Figure 7. The T500 values for these mixes might be influenced by the combined impact of the BA and MK replacements, resulting in better passing ability and lower viscosity. The mixed-type SCCB10M5 had higher flowability, as indicated by the T500 slump flow time decreasing from 3.8 to 3.5 s. The duration increased to 4.1 s for the SCCB10M10 combination while remaining within the EFNARC range. The slump flow time increased by 26.3% when GF was added to SCC at a rate of 0.1%. Incorporating 0.1% of GF, an increase of 17.14% was observed in the SCCB10M5 sump flow time. Adding fiber typically decreases the freshness of concrete (Zeyad, 2020).

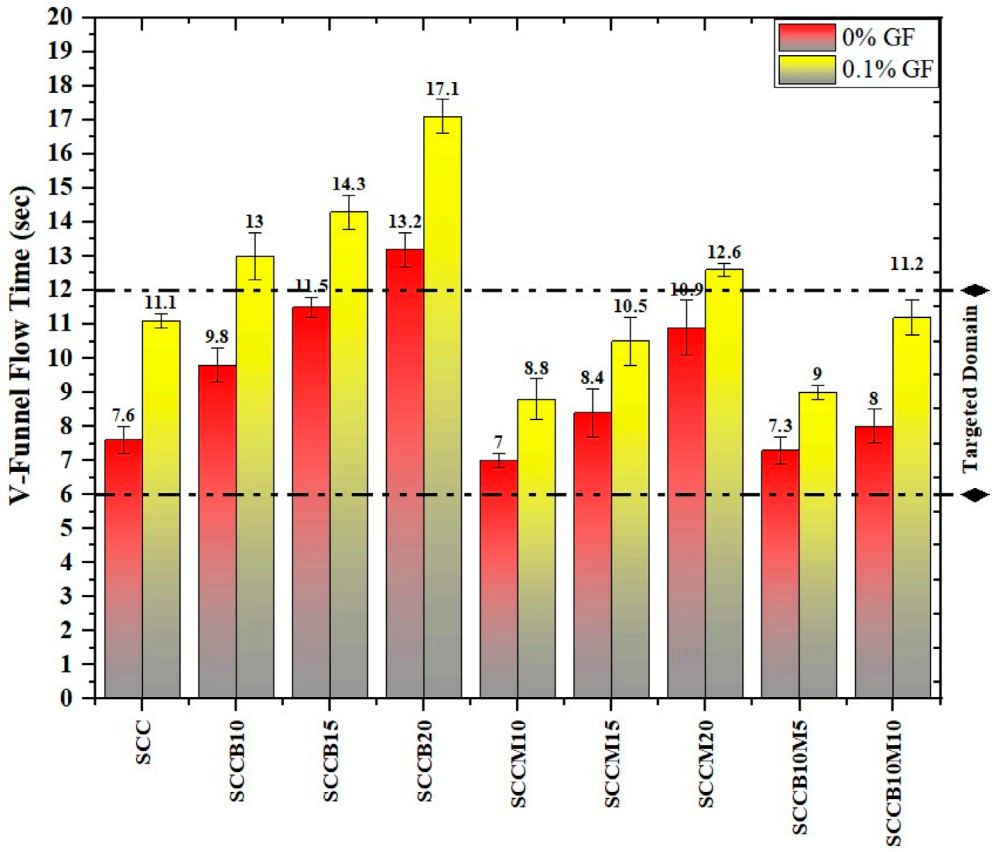

FIGURE 8
Variation in V-funnel flow time for developed SCC.

4.1.3 V-funnel test

The duration required for concrete to pass through V-shaped equipment is the V-funnel flow time. It serves as a gauge for the flowability and viscosity of the concrete mixture. As shown in Figure 8, the V-funnel test time was recorded for 7–13.2 s without using GF. When 0.1% GF was incorporated, the V-funnel flow time increased, revealing that concrete became more viscous and flow-resistant. The V-funnel flow time values increased from SCC to SCCB20 as the proportion of the BA replacement increased. This demonstrated that larger amounts of BA replacement caused concrete to become more viscous and less able to flow. For the SCC mixes containing MK as a 10% substitute for cement, the V-funnel flow time values were lower, and after that, they increased. According to Gill and Siddique (2017), MK increased the workability to 5% cement substitution. Figure 8 shows the timing of the V funnel as observed throughout 8.8–17.1 s using 0.1% GF.

By adding a small quantity of the superplasticizer, mixes prepared with BA, MK, and 0.1% GF collectively all had V-funnel durations within the permissible range. GF decreased the flowability of SCC by lengthening the V-funnel time when added to different blended mixtures. SCCB10M5 was the best combination for the V-funnel timing. The combined impact of the BA and MK substitutes affected the V-funnel flow period for these mixtures, leading to improved flow characteristics. The V-funnel flow times increased with an increase in the GF volume percentage from 0% to 1.5% (Güneyisi et al., 2019). A strong coefficient of determination (R^2 = 0.9162) was used to indicate the link between the V-funnel and T500 time in Figure 9.

4.1.4 L-box test

The L-box test determines the ability of a product to push through densely packed reinforcement on its weight. As shown in Figure 10, the H_2-to-H_1 ratio ranged from 0.7 to 0.93 for SCC combined with BA, MK, and 0.1% GF. As the fraction of the BA replacement increased, the blocking ratio decreased. The SCCB10, SCCB15, and SCCB20 mixes had lower blocking ratios than the control mix (SCC). The lower blocking ratio implied that these blends had less flowability and more inclination to block. The addition of MK to SCC displayed a better result, up to 10% replacement of cement. The blocking ratio for the SCC mixtures was slightly reduced by the addition of 0.1% GF. The blocking ratio for SCCB10M5 increased from 0.91 to 0.93. With the addition of 0.1% GF, the blocking ratio decreased by 8.8% and 2.15% for the SCC and SCCB10M5 mixes, respectively. Compared with the other mix configurations, the SCCB10M5 and SCCB10M10 mixes exhibited comparable blocking ratio values. Figure 11 shows the good linear relationship of the slump flow with the V-funnel (R^2 = 0.8876) and blocking ratio (R^2 = 0.8467). Hassan et al. (2012) described

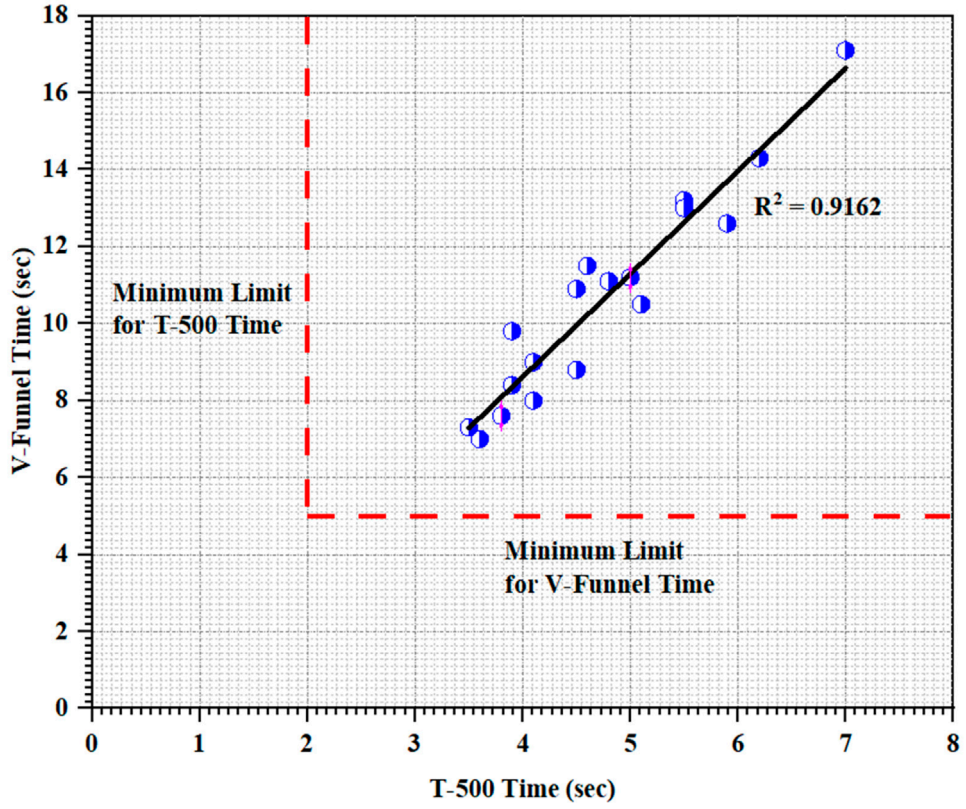

FIGURE 9
Relationship between T500 and V-funnel time.

that the passing ability of the SCC combinations was enhanced by MK. The values of H_2/H_1 increased from 0.63 to 0.89 as the MK content increased from 0% to 25%, demonstrating the improved passing ability.

The findings of the fresh properties showed that the use of BA and MK impacted workability. Compared with the control mix, adding BA to the mixes seemed to reduce their flowability. By increasing the tiny dosage of the water-lowering admixture, the small workability reduction caused by adding BA up to 10% can be enhanced. MK enhanced the workability and passing ability of the SCC mixtures up to 10% replacement of cement. Using BA and MK as cement replacements in the production of SCC is beneficial. Regarding workability, the ideal combination was SCCB10M5, which was achieved by increasing the dosage of the water-reducing additive. Therefore, for further research, SCCB10M5 and SCCB10M10 mixes with and without 0.1% of GF were selected.

4.2 Strength properties of SCC

4.2.1 CS

According to IS 516 (Bureau of Indian Standards BIS, 2021), the CS test was conducted on samples of 150-mm cubes at 7, 14, 28, and 56 days. Figure 12 presents the range of CS across all the concrete blends. At 7, 14, 28, and 56 days, the control mix reached CSs of 36 MPa, 44.20 MPa, 54 MPa, and 57.20 MPa, respectively. The strength values for the BA-, MK-, and GF-blended SCC mixes were comparable and even superior to those of the control SCC mix. SCC1M20 performed better at 7 days, with the highest CS of 40.20 MPa, whereas SCC1B10M5 measured the highest CS of 64.50 MPa at 56 days. The strength was enhanced by 3.1% for SCCB10 at 28 days and 3.5% at 56 days compared with the control mix. For mixes prepared using MK instead of cement, SCCM15 attained 28-day and 56-day strengths of 57.05 MPa and 61.55 MPa, respectively, which were 5.6% and 7.6% higher than those of the control mix. The BA and MK optimal percentages of cement were 10% and 15%, respectively. The outcomes of the tests showed that when BA and MK were added to concrete, the CS of the mixture improved. The strength of the SCCB10M5 mixture was 62.60 MPa, which was 9.4% higher than that of the control mixture. Compared with the control mix, the strength of the SCC1B10M5 mix increased by 12.8% with the addition of 0.1% GF. The concrete mixes with SCCB10M5 and SCCB10M10 proportions had CSs of 62.6 MPa and 60 MPa, respectively, and increases in CSs of 9.4% and 4.9%, respectively, compared with the control mix. CS was enhanced by 1.5%–3.4% with the addition of 0.1% GF. Because of the pozzolanic behavior of BA and MK, this issue provided unequivocal evidence for the growth of the strength with age. The characteristics of the hardened concrete were considerably improved by the addition of MK (Meraz et al., 2023). CS was more positively impacted by MK (Dadsetan and Bai, 2017).

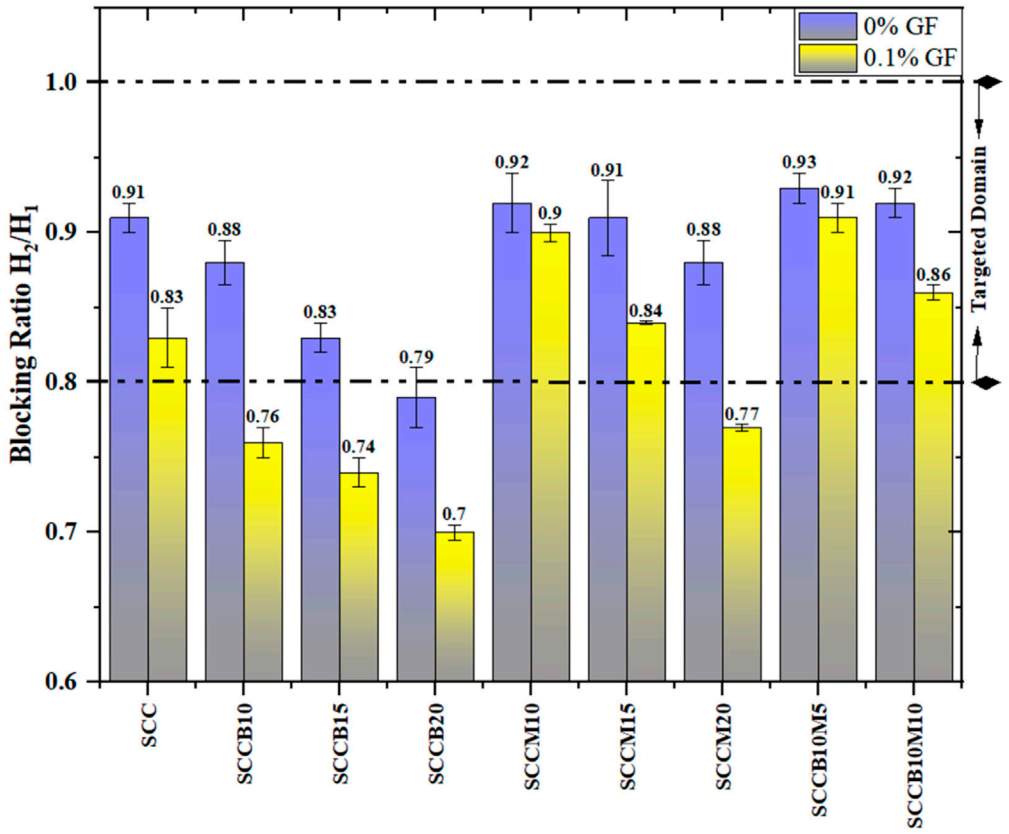

FIGURE 10
Comparison of blocking ratio for developed SCC.

4.2.2 FS

Figure 13 depicts the variations in FS for all the developed SCC mixes. FS was assessed after 7, 28, and 56 days of curing, and the values were predicted using the mean of three specimens. The results of these tests were calculated using IS 516 (Bureau of Indian Standards BIS, 2021). FS is assessed using beams with a flexural testing apparatus with two-point loading. According to IS 456 (Bureau of Indian Standards BIS, 2000), the minimum FS recommended for concrete is 0.7 times the square root of its typical CS. The greatest FS of 5.30 MPa was recorded for SCC1M15 at 7 days, whereas the highest strength of 8.80 MPa was recorded for SCC1B10M5 at 56 days. FS measured in the 56-day samples was increased for the mix groups of SCCB10, SCCB15, SCCB20, SCC1B10, SCC1B15, SCC1B20, SCCM10, SCCM15, SCCM20, SCC1M10, SCC1M15, and SCC1M20 by 5.7%, 2.9%, −4.3%, 15.7%, 10%, −2.1%, 9.3%, 12.1%, 1.4%, 19.3%, 22.9%, and 2.9%, respectively. Compared with the control mix, SCCB10M5 and SCCB10M10 had greater FS of 7.90 MPa and 7.65 MPa at 56 days, respectively. However, compared with the control mix, SCCB10M5 and SCCB10M10 indicated a considerable enhancement in FS after 56 days, with percentage increases of approximately 12.9% and 9.3%, respectively. For SCC containing 0.1% GF, FS increased by 5.9%–11.4% at 56 days. The maximum strength was measured for the SCC1B10M5 mix at 8.80 MPa, which was enhanced by 25.7% compared with the reference SCC mix. Bheel et al. (2021) reported that 10% cement substitution by MK increased FS by 13%.

4.2.3 STS

Figure 14 represents the variation in STS for all the developed SCC mixes. STS was computed using cylinders of 150-mm diameter, and the mean of three specimens was used to determine STS for each mix. To assess the strength, references were made to IS 516 (Bureau of Indian Standards BIS, 2021) and IS 5816 (Bureau of Indian Standards, 1999). The STS values of the control mix (SCC) samples at 7, 14, 28, and 56 days were 3.30, 4.30, 5.15, and 5.85 MPa, respectively. Similar to FS, when BA and MK were utilized collectively in place of cement, STS increased approximately between 6% and 11.1%. The SCC1B10M5 mix had the highest strength of 7.15 MPa, which was enhanced by 22.2% compared with the reference SCC mix. When coupled with the control mix, the strength increases for SCCB10M5 and SCCB10M10 were 11.1% and 6%, respectively. For SCC containing 0.1% GF, STS increased by 10%–12.8% at 56 days. It was discovered that all the mixtures with STS-to-CS ratios fell between 1/10 and 1/11. Figure 15 shows a detailed comparison of the CS, STS, and FS of the developed SCC. This figure illustrates that CS had a good linear relationship with both FS (R^2 = 0.8724) and STS (R^2 = 0.7399). The following equations (Equations 3, 4) were developed

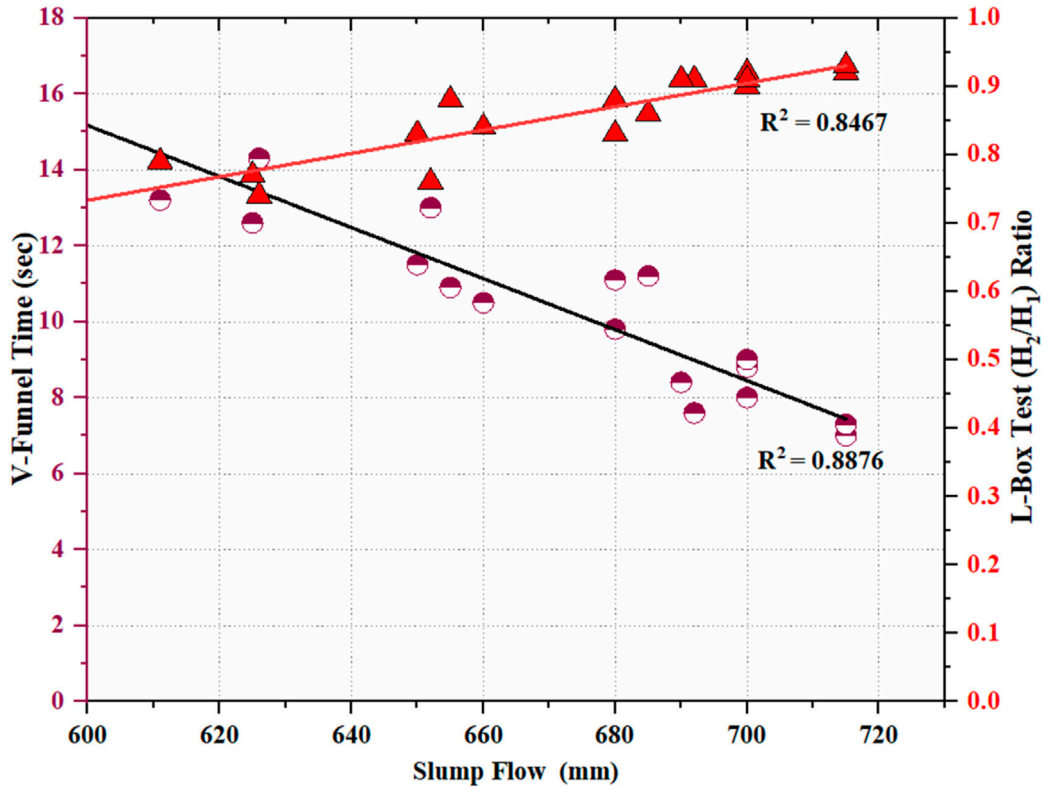

FIGURE 11
Comparison of slump flow versus V-funnel time and blocking ratio.

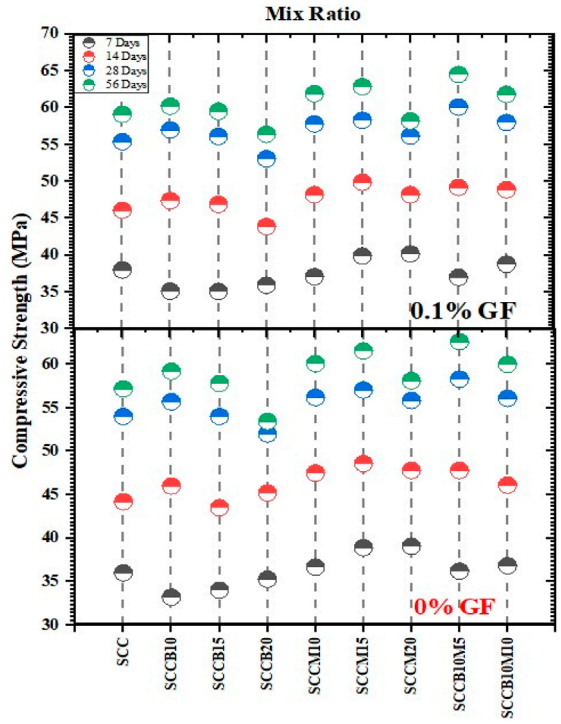

FIGURE 12
Comparison of CS of developed SCC.

to correlate the relationship between the CS and FS and STS of the developed SCC mixes.

$$FS = 0.0111\,CS^{1.5982}, \tag{3}$$

$$STS = 0.06\,CS^{1.14}. \tag{4}$$

5 UPV of SCC samples

Figure 16 presents the UPV outcomes for the SCC samples blended with BA and MK at 56 days as per IS 13311 (Bureau of Indian Standards BIS, 1992) compared with CS. It has been established that concrete with a higher UPV may also have a higher CS and *vice versa*, although not always. The findings of the study revealed that there was an increment in UPV with the addition of BA and MK to the mixture. In the research, UPV values for all the developed SCC mixes were in the range of 4,100 m/s–4,850 m/s. SCCB10M5 and SCCB10M10 showed excellent quality concrete, and all other SCC mixes demonstrated good quality concrete. As the BA and MK contents in the mixture increased, UPV also increased. At 56 days of normal water curing, the increases in UPV were 12.5% and 9.1% for SCCB10M5 and SCCB10M10, respectively, and with the addition of 0.1% GF, UPV was enhanced between 3% and 5.9%. At 56 days, the maximum UPV was measured for SCC1B10M5, approximately 16% higher than that of the control

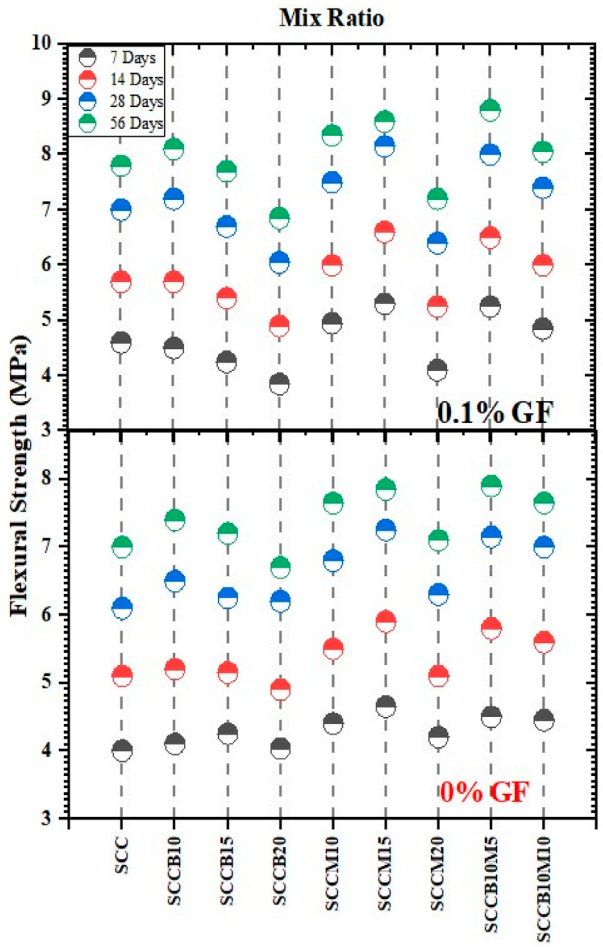

FIGURE 13
Variation in FS of developed SCC.

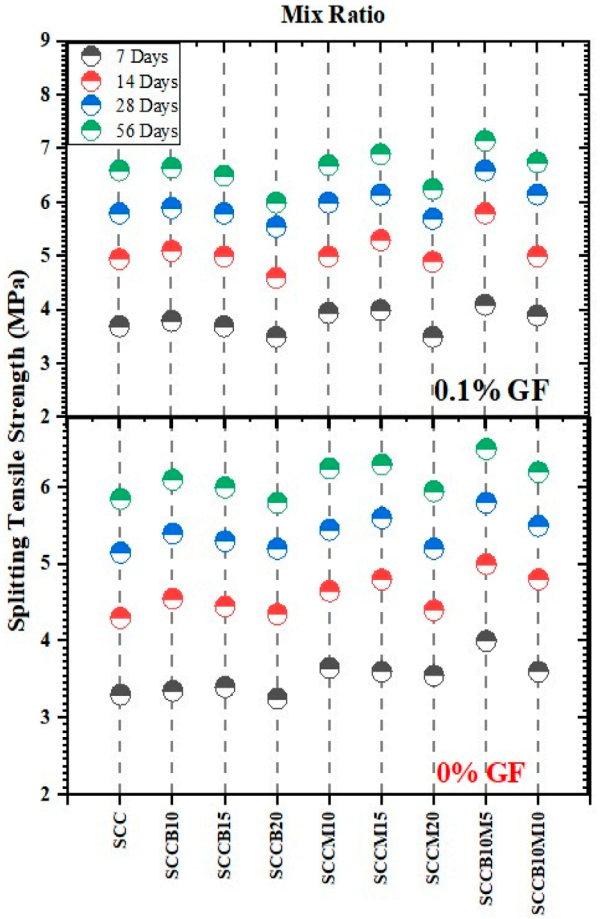

FIGURE 14
Variation in STS of developed SCC.

mix (SCC). Figure 16 depicts the relationship between UPV and CS. A best-fit curve using an exponential formula (Equation 5) well represents the correlation between the two parameters, with an R^2 value of 0.928. Supplementary Figure S4 displays testing of the developed SCC.

$$CS = 28.37e^{0.0002UPV}. \quad (5)$$

5.1 Sulfuric acid attack test on SCC

To verify the resistance of the developed SCC mixtures against sulfate attack, a sulfuric acid attack test was also conducted. Following a 28-day curing period in regular water, the developed SCC samples were submerged in a 3% H_2SO_4 solution for up to 56 days. After 56 days of immersion in the 3% H_2SO_4 solution, the weight loss and UPV and RCPT charges passed were evaluated. Figure 17 indicates the weight loss of the developed SCC samples blended with BA, MK, and GF content against sulfuric acid attack at 7, 14, 28, and 56 days. The weight loss for the control sample after 56 days of immersion in a sulfuric acid solution was 4.01%. For SCCB10M5 and SCCB10M10, the weight losses were 1.14% and 1.01%, respectively. After incorporating 0.1% GF, weight loss was reduced. The minimum weight loss was noted at 1.01% for SCC1B10M5. Figure 18A provides the outcomes for the UPV of the SCC samples blended with BA and MK with and without sulfuric acid. At 56 days of normal water curing, the increases in UPV were 12.5% and 9.1% for SCCB10M5 and SCCB10M10, respectively. With the addition of 0.1% GF, UPV was enhanced by between 3% and 5.9%. After immersion in sulfuric acid, the increases in UPV were 20.6% and 13.9% for SCCB10M5 and SCCB10M10, respectively, compared with the control mix at 56 days. The maximum decrease in UPV was noted at 12.2% for the control mix, and the minimum was 3.1% for SCC1B10M5 after the effect of sulfuric acid compared with the normal water curing. The presence of BA, MK, and GF remarkably enhanced the resistance to sulfuric acid attack.

To establish the resistance of a specimen to chloride ions entering concrete, the RCPT is often used following ASTM-C1202 (ASTM, 2024). Analyzing the number of charges transmitted exhibits the concrete quality. The actual charge that chloride penetration transmits for every SCC is shown in Figure 18B. There were approximately 1,000–1,325 coulombs after 56 days of curing. The results showed that the SCC1BA10M5 combination had the

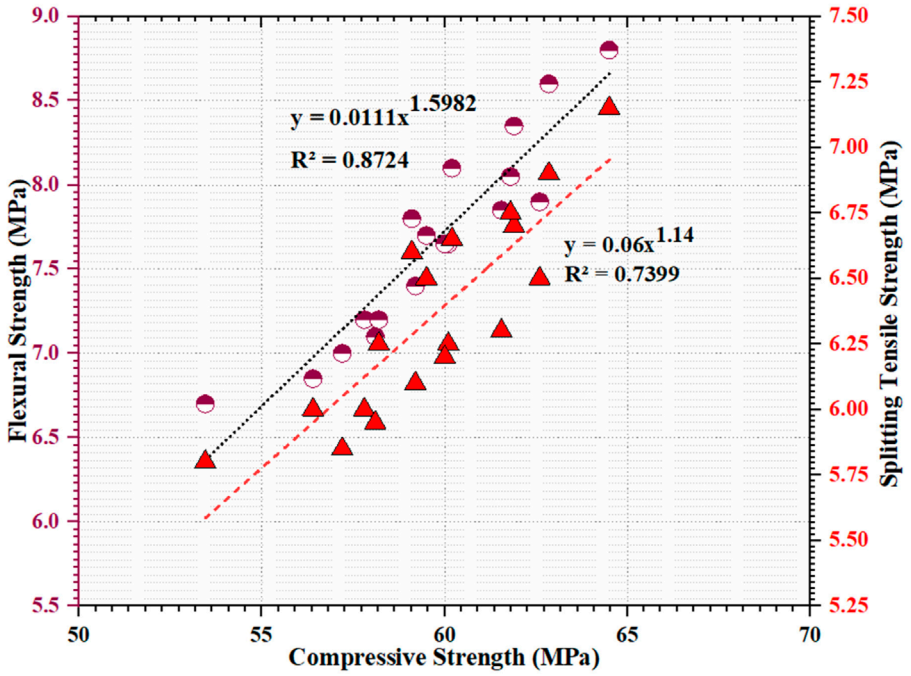

FIGURE 15
Comparison of CS versus FS and STS of developed SCC.

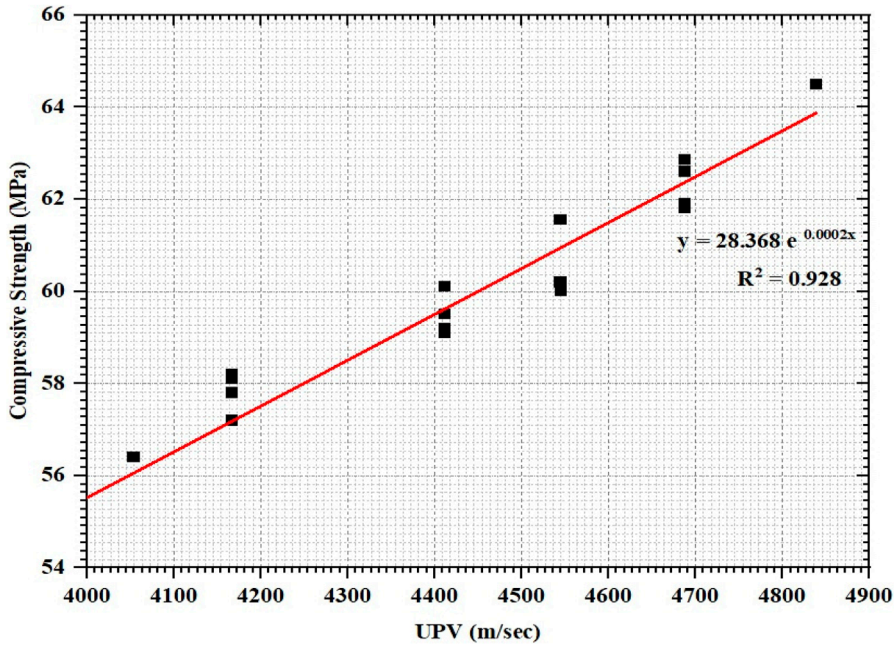

FIGURE 16
Correlation of UPV with CS.

lowest amount of charge passing through it among all the mixes (1,000 coulombs), which implied that the blend was more durable.

Compared with the control mix, the proportion of passed coulomb charges decreased by 16.2%, 12.8%, 24.5%, and 13.2% in SCCB10M5, SCCB10M10, SCC1B10M5, and SCC1B10M10, respectively. After immersion in 3% of H_2SO_4 solution, the decreases in the percentage of charge passed were 20.4%, 16.1%, 29.4%, and 15.4% for SCCB10M5, SCCB10M10,

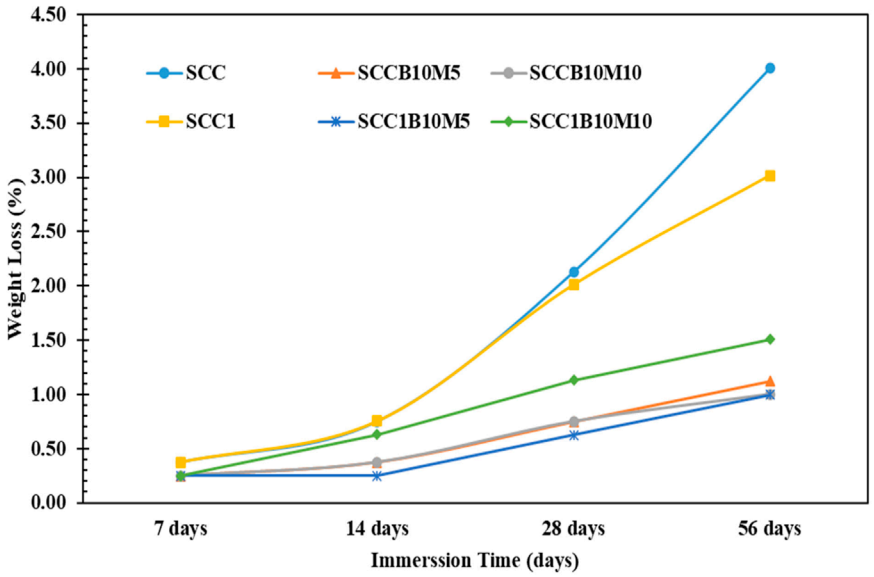

FIGURE 17
Weight loss versus acid attack in developed SCC.

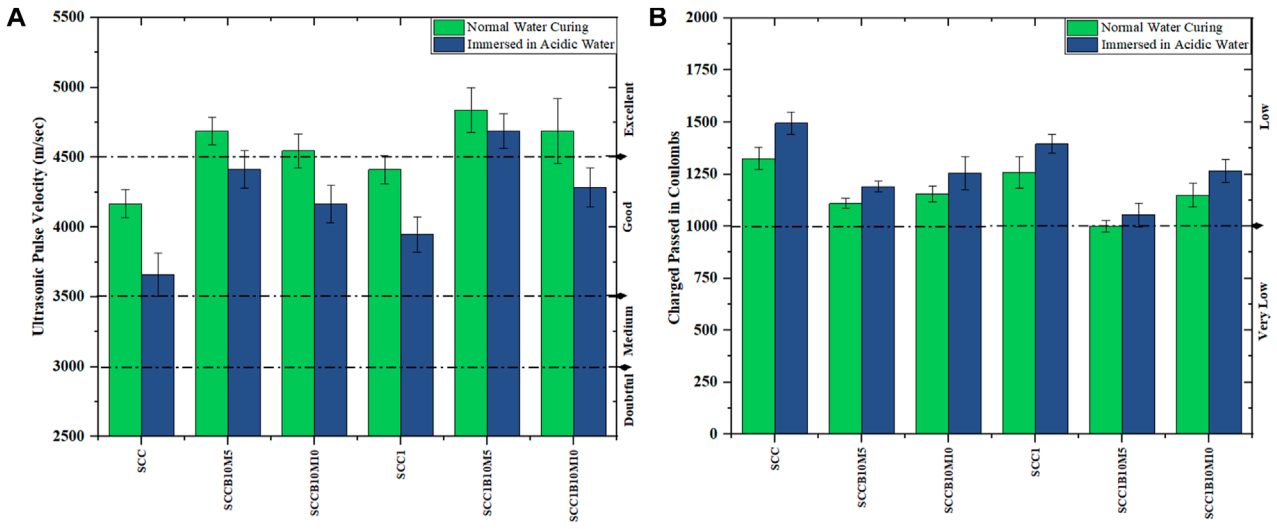

FIGURE 18
(A) UPV versus acid attack and **(B)** RCPT versus acid attack of developed SCC.

SCC1B10M5, and SCC1B10M10, respectively, compared to the control mix.

6 Microstructural properties of SCC

The control mix (SCC) and SCC1B10M5 underwent microstructural investigation to elucidate the mechanism underlying the degradation of the SCC specimens by sulfate attack. This was done to determine whether the SCC specimens were susceptible to sulfate attack. To determine the elemental composition, energy-dispersive X-ray (EDX) analysis was performed. The image demonstrated that the control sample, a combination of BA and MK, had voids, tiny holes, and microcracks. Comparing the SCC performance with mixes that included BA and MK, it might be concluded that SCC performed poorly. Figure 19A displays the voids and microcracks. However, a more homogenous structure was detected in the data for mixes containing BA and MK, as shown in Figure 19C. The pores were significantly reduced by the small size of the MK and BA particles. In the SCC mixed with MK and BA, no voids were detected (Figure 19C). This factor helped increase the strength characteristics of the MK and BA SCC. The C-S-H gel was observed in the SEM images of SCC1B10M5. This C-S-H gel formation reduced the voids even further and

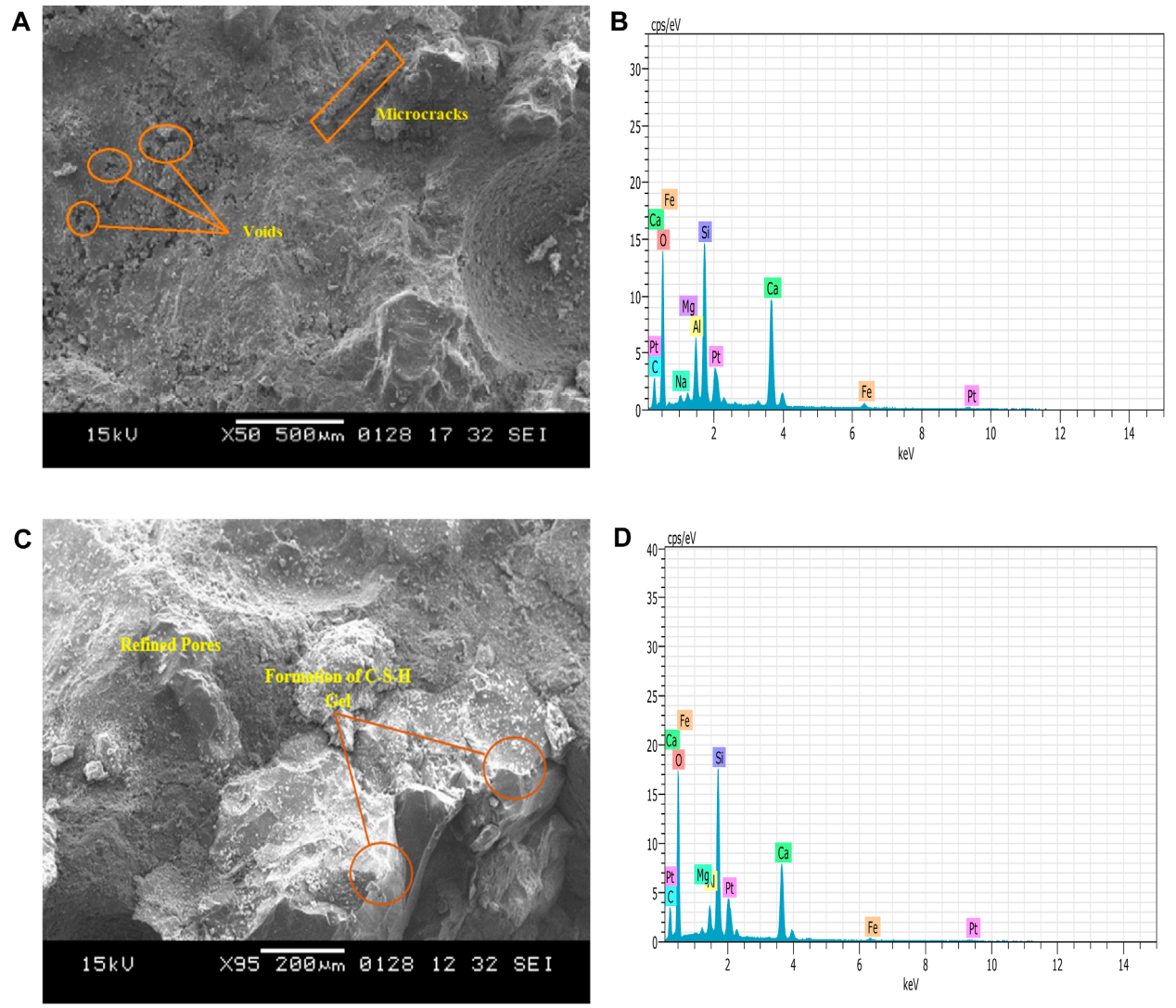

FIGURE 19
(A) SEM image of SCC control mix, **(B)** EDX image of SCC control mix, **(C)** SEM image of SCC1B10M5, and **(D)** EDX image of SCC1B10M5.

enhanced the strength. The elemental composition was determined by EDX analysis. The EDX study (Figures 19B, D) depicted that the BA- and MK-blended SCC (SCC1B10M5) had a higher silica content than the control SCC. The greater silica concentration suggested that the SCC1B10M5 mix had a positive pozzolanic reaction and synergistic impact (Kannan and Ganesan, 2014). In addition, the atomic Ca-to-Si ratios for the control and BA- and MK-blended SCC mixes were calculated. The results revealed that the atomic Ca-to-Si ratio of the control SCC mix was 1.13, whereas it was lowered to 0.773 in the BA- and MK-blended SCC (SCC1B10M5). The enhancement in the macro-level features of SCC was reflected in the decrease in this value. The primary factor for the reduction in the Ca-to-Si ratio was the conversion of CH to secondary C-S-H. Secondary C-S-H was produced as a consequence of this reaction, and by adjusting the pore structure and lowering the overall porosity, it increased strength and impermeability (Poon et al., 2006).

6.1 Comparative analysis

Table 2 presents the comparative analysis of previous studies using BA and MK as SCMs for the various fresh and strength properties of SCC. All the studies mentioned the result without the effect of sulfuric acid attack. The current investigation, which used BA and MK both individually and in combination, demonstrated the freshness and strength properties and the effect of immersion of the specimen in sulfuric acid on weight loss, UPV, and RCPT.

6.2 Conclusion

This study showed that BA and MK can replace cement as the main binder in concrete production because of their pozzolanic properties. Based on these results, the primary conclusions from this study were as follows:

TABLE 2 Comparative analysis of SCC.

SCM	Replacement percentage (%)	SP %	Slump flow (mm)	V-funnel time (sec)	Blocking ratio (H_2/H_1)	CS (28 days) (MPa)	FS (28 days) (MPa)	STS (28 days) (MPa)	Immersion in acidic water (AW)	Weight loss in AW% at 28 days	UPV in AW (m/sec)	Reference
BA and BFS	0%–20% @ 10%	1.4	650	9.52	------	34	------	------	------	------	------	Le et al. (2018)
BA	0%–25% @ 5%	4.5	------	5.3	0.93	63	------	4.7	------	------	------	Zareei et al. (2018)
MK	0%–25% @ 5%	2.3	730	8	0.98	55	------	4.81	------	------	------	Vivek and Dhinakaran (2017)
MK	0%–15% @ 5%	1.63	710	4.5	0.83	40.1	4	2.1	------	------	------	Karahan et al. (2012)
MK	0%–15% @ 5%	2	755	8	0.9	52.40	------	4.43	------	------	------	Gill and Siddique (2017)
MK	3%, 5%, 8%, 11%, 15%, and 20%	0.8 to 1.1	650	8	0.89	48.9	------	------	------	------	------	Hassan et al. (2012)
MK and GSA	0%–20% @ 5% 0%–100% @ 2.5%	3	700	10.2	0.96	57	5.2	4.7	------	------	------	Bheel et al. (2021)
MK	0%–25% @ 5%	2	720	4.5	0.9	57	------	------	5% H_2SO_4	3	------	Kannan and Ganesan (2014)
BA & MK + 0.1% GF	0%, 10% & 0%, 5%, and 10%	1.9	715	7	0.93	60.10	8.15	6.60	3% H_2SO_4	0.63	4,688	This study

BA, bagasse ash; MK, metakaolin; BFS, blast furnace slab; GSA, groundnut shell ash; GF, glass fiber; SP, superplasticizer; CS, compressive strength; FS, flexural strength; STS, splitting tensile strength; UPV in NW, ultrasonic pulse velocity in normal water curing; UPV in AW, UPV in acidic water.

10.3389/fmats.2024.1351554

- BA and MK, when used together as a cement alternative up to 15%, are beneficial in developing SCC. Adding BA to mixtures appeared to reduce the flowability as the amount of BA increased; however, adding MK enhanced the flowability up to 10% cement substitution.
- A slight increase in the water-reducing admixture dosage improved the filling and passing ability of SCC combined with BA and MK. SCCB10M5 was the most workable SCC combination, with a slight increase in the water-reducing admixture dosage. The workability of SCC decreased with 0.1% GF but remained within the EFNARC guidelines. A strong linear relationship was observed between the slump flow values (mm) and V-funnel duration (sec), with $R^2 = 0.8876$, and the blocking ratio (H_2/H_1), with $R^2 = 0.8467$.
- Higher CS, FS, and STS values were observed when cement was replaced with up to 15% BA and MK along with 0.1% GF. SCC1B10M5 exhibited the highest strength throughout all the testing ages. At 56 days, the SCC1B10M5 mix had 12.8%, 25.7%, and 22.2% higher CS, FS, and STS than the control mix, respectively. An exponential best-fit curve revealed a link between the CS and UPV, as evidenced by the strong coefficient of determination ($R^2 = 0.928$).
- Sulfate resistance was substantially improved by BA, MK, and GF, as evidenced by weight loss. When SCC1B10M5 was compared with the control mix, the weight loss decreased from 4.01% to 1.01%. After 56 days, SCC1B10M5, which generated superior concrete, reduced chloride ion penetration by 24.5% and 29.4%, respectively, when cured in standard water and immersed in sulfuric acid. Cracks were observed at the contact surface of the control mix, and refined apertures were identified in the SCC1B10M5 concrete mixture, as determined by the microstructural analysis. This distinction between the two mixtures increased the mechanical strength. Low Ca/Si ratios increased CS, as determined by the EDX results.

Data availability statement

The raw data supporting the conclusion of this article will be made available by the authors, without undue reservation.

Author contributions

MW: conceptualization, formal analysis, investigation, methodology, validation, and writing–original draft. UW: conceptualization, formal analysis, investigation, methodology, validation, and writing–original draft. AB: conceptualization, formal analysis, investigation, methodology, resources, validation, writing–original draft, and writing–review and editing. KA: conceptualization, formal analysis, investigation, methodology, validation, and writing–original draft. YÖ: investigation, validation, and writing–original draft. AN: formal analysis, validation, and writing–original draft.

Funding

The author(s) declare that no financial support was received for the research, authorship, and/or publication of this article.

Conflict of interest

The authors declare that the research was conducted in the absence of any commercial or financial relationships that could be construed as a potential conflict of interest.

Publisher's note

Supplementary material

The Supplementary Material for this article can be found online at: https://www.frontiersin.org/articles/10.3389/fmats.2024.1351554/full#supplementary-material

References

Abed, M., Rashid, K., Rehman, M. U., and Ju, M. (2022). Performance keys on self-compacting concrete using recycled aggregate with fly ash by multi-criteria analysis. *J. Clean. Prod.* 378, 134398. doi:10.1016/j.jclepro.2022.134398

Agrawal, D., Waghe, U., Ansari, K., Dighade, R., Amran, M., Qader, D. N., et al. (2023). Experimental effect of pre-treatment of rubber fibers on mechanical properties of rubberized concrete. *J. Mater. Res. Technol.* 23, 791–807. doi:10.1016/j.jmrt.2023.01.027

Ahmad, S., and Umar, A. (2018). Rheological and mechanical properties of self-compacting concrete with glass and polyvinyl alcohol fibres. *J. Build. Eng.* 17, 65–74. doi:10.1016/j.jobe.2018.02.002

Ahmad, S., Umar, A., and Masood, A. (2017). "Properties of normal concrete, self-compacting concrete and glass fibre-reinforced self-compacting concrete: an experimental study," in *Procedia eng* (Elsevier Ltd), 807–813. doi:10.1016/j.proeng.2016.12.106

Ahmad, W., Ahmad, A., Ostrowski, K. A., Aslam, F., Joyklad, P., and Zajdel, P. (2021). Sustainable approach of using sugarcane bagasse ash in cement-based composites: a systematic review. *Case Stud. Constr. Mater.* 15, e00698. doi:10.1016/j.cscm.2021.e00698

Akhmetov, D., Akhazhanov, S., Jetpisbayeva, A., Pukharenko, Y., Root, Y., Utepov, Y., et al. (2022). Effect of low-modulus polypropylene fiber on physical and mechanical properties of self-compacting concrete. *Case Stud. Constr. Mater.* 16, e00814. doi:10.1016/j.cscm.2021.e00814

Akram, T., Memon, S. A., and Obaid, H. (2009). Production of low cost self compacting concrete using bagasse ash. *Constr. Build. Mater* 23, 703–712. doi:10.1016/j.conbuildmat.2008.02.012

Aksoylu, C., Ozkılıç, Y. O., Bahrami, A., Yıldızel, S. A., Hakeem, I. Y., Ozdöner, N., et al. (2023). Application of waste ceramic powder as a cement replacement in reinforced concrete beams toward sustainable usage in construction. *Case Stud. Constr. Mater.* 19, e02444. doi:10.1016/j.cscm.2023.e02444

Alola, A. A., Bekun, F. V., Adebayo, T. S., and Uzuner, G. (2023). The nexus of disaggregated energy sources and cement production carbon emission in China. *Energy & Environ.* 34, 1937–1956. doi:10.1177/0958305X221102047

Amin, M., Attia, M. M., Agwa, I. S., Elsakhawy, Y., el-hassan, K. A., and Abdelsalam, B. A. (2022). Effects of sugarcane bagasse ash and nano eggshell powder on high-strength concrete properties. *Case Stud. Constr. Mater.* 17, e01528. doi:10.1016/j.cscm.2022.e01528

Antoun, M., Issa, C. A., Aouad, G., and Gerges, N. (2021). Sustainable masonry blocks: olive wood waste as substitute for fine aggregates. *Case Stud. Constr. Mater.* 15, e00590. doi:10.1016/j.cscm.2021.e00590

Asteris, P. G., Lourenço, P. B., Roussis, P. C., Elpida Adami, C., Armaghani, D. J., Cavaleri, L., et al. (2022). Revealing the nature of metakaolin-based concrete materials using artificial intelligence techniques. *Constr. Build. Mater* 322, 126500. doi:10.1016/j.conbuildmat.2022.126500

ASTM (2024) *Standard test method for electrical indication of concrete's ability to resist chloride ion penetration*. ASTM-C1202. West Conshohocken, Pennsylvania, United States: ASTM. doi:10.1520/C1202-12

Bai, B., Chen, J., Bai, F., Nie, Q., and Jia, X. (2024). Corrosion effect of acid/alkali on cementitious red mud-fly ash materials containing heavy metal residues. *Environ. Technol. Innov.* 33, 103485. doi:10.1016/j.eti.2023.103485

Bheel, N., Awoyera, P., Tafsirojjaman, T., Hamah Sor, N., and sohu, S. (2021). Synergic effect of metakaolin and groundnut shell ash on the behavior of fly ash-based self-compacting geopolymer concrete. *Constr. Build. Mater* 311, 125327. doi:10.1016/j.conbuildmat.2021.125327

Bureau of Indian standards (1999). *Specification for splitting tensile strength of concrete -method of test*. New Delhi, India: BIS. IS 5816-1999.

Bureau of Indian Standards (BIS) (1992). *Method of Non-destructive testing of concret, Part 1: ultrasonic pulse velocity*. New Delhi, India. IS 13311-1.

Bureau of Indian Standards (BIS) (2000). *Plain and reinforced concrete - code of practice*. New Delhi, India: BIS. IS 456-2000.

Bureau of Indian standards (BIS) (2013). *Specification for 43 grade ordinary Portland cement*, New Delhi, India: BIS. IS 8112-2013.

Bureau of Indian standards (BIS) (2016). *Coarse and fine aggregate for concrete - specification*. New Delhi, India: BIS, 383–2016. Available at: www.standardsbis.in.

Bureau of Indian Standards (BIS) (2021). *Hardened concrete - methods of test. vol. 54*. IS 516-2021. New Delhi, India: BIS. Available at: www.standardsbis.in.

Celik, A. I., Ozkılic, Y. O., Bahrami, A., and Hakeem, I. Y. (2023a). Effects of glass fiber on recycled fly ash and basalt powder based geopolymer concrete. *Case Stud. Constr. Mater.* 19, e02659. doi:10.1016/j.cscm.2023.e02659

Celik, A. I., Ozkilic, Y. O., Bahrami, A., and Hakeem, I. Y. (2023b). Mechanical performance of geopolymer concrete with micro silica fume and waste steel lathe scraps. *Case Stud. Constr. Mater.* 19, e02548. doi:10.1016/j.cscm.2023.e02548

Chen, L., Chen, Z., Xie, Z., Wei, L., Hua, J., Huang, L., et al. (2023). Recent developments on natural fiber concrete: a review of properties, sustainability, applications, barriers, and opportunities. *Dev. Built Environ.* 16, 100255. doi:10.1016/j.dibe.2023.100255

Dadsetan, S., and Bai, J. (2017). Mechanical and microstructural properties of self-compacting concrete blended with metakaolin, ground granulated blast-furnace slag and fly ash. *Constr. Build. Mater* 146, 658–667. doi:10.1016/j.conbuildmat.2017.04.158

Danish, P., and Mohan Ganesh, G. (2021). "Study on influence of Metakaolin and waste marble powder on self-compacting concrete - a state of the art review," in *Mater today proc* (Elsevier Ltd), 1428–1436. doi:10.1016/j.matpr.2020.11.629

Das, D., Saravanan, T. J., Bisht, K., and Kabeer, K. I. S. A. (2022). A review of fresh properties of self-compacting concrete incorporating sugarcane bagasse ash. *Mater Today Proc.* 65, 852–859. doi:10.1016/j.matpr.2022.03.451

Ding, J.-T. (2002). Effects of metakaolin and silica fume on properties of concrete. Available at: https://www.researchgate.net/publication/279902244.

Domone, P. L. (2007). A review of the hardened mechanical properties of self-compacting concrete. *Cem. Concr. Compos* 29, 1–12. doi:10.1016/j.cemconcomp.2006.07.010

EFNARC (2002). Specification and guidelines for self-compacting concrete. Available at: www.efnarc.org.

Farrant, W. E., Babafemi, A. J., Kolawole, J. T., and Panda, B. (2022). Influence of sugarcane bagasse ash and silica fume on the mechanical and durability properties of concrete. *Materials* 15, 3018. doi:10.3390/ma15093018

Fayed, S., Madenci, E., Bahrami, A., Ozkiliç, Y. O., and Mansour, W. (2023). Experimental study on using recycled polyethylene terephthalate and steel fibers for improving behavior of RC columns. *Case Stud. Constr. Mater.* 19, e02344. doi:10.1016/j.cscm.2023.e02344

Gerges, N. N., Issa, C. A., and Fawaz, S. A. (2018). Rubber concrete: mechanical and dynamical properties. *Case Stud. Constr. Mater.* 9, e00184. doi:10.1016/j.cscm.2018.e00184

Gerges, N. N., Issa, C. A., Khalil, N. J., Abdul Khalek, L., Abdo, S., and Abdulwahab, Y. (2023). Flexural capacity of eco-friendly reinforced concrete beams. *Sci. Rep.* 13, 20142. doi:10.1038/s41598-023-47283-6

Gerges, N. N., Issa, C. A., Sleiman, E., Aintrazi, S., Saadeddine, J., Abboud, R., et al. (2022). Eco-friendly optimum structural concrete mix design. *Sustainability* 14, 8660. doi:10.3390/su14148660

Gill, A. S., and Siddique, R. (2017). Strength and micro-structural properties of self-compacting concrete containing metakaolin and rice husk ash. *Constr. Build. Mater* 157, 51–64. doi:10.1016/j.conbuildmat.2017.09.088

Güneyisi, E., Atewi, Y. R., and Hasan, M. F. (2019). Fresh and rheological properties of glass fiber reinforced self-compacting concrete with nanosilica and fly ash blended. *Constr. Build. Mater* 211, 349–362. doi:10.1016/j.conbuildmat.2019.03.087

Gupta, A., Gupta, N., and Saxena, K. K. (2021). Mechanical and durability characteristics assessment of geopolymer composite (Gpc) at varying silica fume content. *J. Compos. Sci.* 5, 237. doi:10.3390/JCS5090237

Hajali, M., Alavinasab, A., and Abi Shdid, C. (2016). Structural performance of buried prestressed concrete cylinder pipes with harnessed joints interaction using numerical modeling. *Tunn. Undergr. Space Technol.* 51, 11–19. doi:10.1016/j.tust.2015.10.016

Hamza Hasnain, M., Javed, U., Ali, A., and Saeed Zafar, M. (2021). Eco-friendly utilization of rice husk ash and bagasse ash blend as partial sand replacement in self-compacting concrete. *Constr. Build. Mater* 273, 121753. doi:10.1016/j.conbuildmat.2020.121753

Hassan, A. A. A., Lachemi, M., and Hossain, K. M. A. (2012). Effect of metakaolin and silica fume on the durability of self-consolidating concrete. *Cem. Concr. Compos* 34, 801–807. doi:10.1016/j.cemconcomp.2012.02.013

He, H., E, S., Wen, T., Yao, J., Wang, X., He, C., et al. (2023). Employing novel N-doped graphene quantum dots to improve chloride binding of cement. *Constr. Build. Mater* 401, 132944. doi:10.1016/j.conbuildmat.2023.132944

Huang, H., Yuan, Y., Zhang, W., and Zhu, L. (2021). Property assessment of high-performance concrete containing three types of fibers. *Int. J. Concr. Struct. Mater* 15, 39. doi:10.1186/s40069-021-00476-7

Iftikhar, B., Alih, S. C., Vafaei, M., Javed, M. F., Rehman, M. F., Abdullaev, S. S., et al. (2023). Predicting compressive strength of eco-friendly plastic sand paver blocks using gene expression and artificial intelligence programming. *Sci. Rep.* 13, 12149. doi:10.1038/s41598-023-39349-2

Issa, C. A., and Salem, G. (2013). Utilization of recycled crumb rubber as fine aggregates in concrete mix design. *Constr. Build. Mater* 42, 48–52. doi:10.1016/j.conbuildmat.2012.12.054

Jahami, A., and Issa, C. A. (2023). Exploring the use of mixed waste materials (MWM) in concrete for sustainable Construction: a review. *Constr. Build. Mater* 398, 132476. doi:10.1016/j.conbuildmat.2023.132476

Kannan, V., and Ganesan, K. (2014). Chloride and chemical resistance of self compacting concrete containing rice husk ash and metakaolin. *Constr. Build. Mater* 51, 225–234. doi:10.1016/j.conbuildmat.2013.10.050

Karahan, O., Hossain, K. M. A., Ozbay, E., Lachemi, M., and Sancak, E. (2012). Effect of metakaolin content on the properties self-consolidating lightweight concrete. *Constr. Build. Mater* 31, 320–325. doi:10.1016/j.conbuildmat.2011.12.112

Kumar Jagarapu, D. C., and Eluru, A. (2020). "Strength and durability studies of lightweight fiber reinforced concrete with agriculture waste," in *Mater today proc* (Elsevier Ltd), 914–919. doi:10.1016/j.matpr.2020.01.257

Larissa, L. C., Marcos, M. A., Maria, M. V., de Souza, N. S. L., and de Farias, E. C. (2020). Effect of high temperatures on self-compacting concrete with high levels of sugarcane bagasse ash and metakaolin. *Constr. Build. Mater* 248, 118715. doi:10.1016/j.conbuildmat.2020.118715

Le, D. H., Sheen, Y. N., and Lam, M. N. T. (2018). Fresh and hardened properties of self-compacting concrete with sugarcane bagasse ash–slag blended cement. *Constr. Build. Mater* 185, 138–147. doi:10.1016/j.conbuildmat.2018.07.029

Li, Z., Gao, M., Lei, Z., Tong, L., Sun, J., Wang, Y., et al. (2023). Ternary cementless composite based on red mud, ultra-fine fly ash, and GGBS: synergistic utilization and geopolymerization mechanism. *Case Stud. Constr. Mater.* 19, e02410. doi:10.1016/j.cscm.2023.e02410

Lin, J.-X., Chen, G., Pan, H., Wang, Y., Guo, Y., and Jiang, Z. (2023). Analysis of stress-strain behavior in engineered geopolymer composites reinforced with hybrid PE-PP fibers: a focus on cracking characteristics. *Compos Struct.* 323, 117437. doi:10.1016/j.compstruct.2023.117437

Madurwar, M. V., Ralegaonkar, R. V., and Mandavgane, S. A. (2013). Application of agro-waste for sustainable construction materials: a review. *Constr. Build. Mater* 38, 872–878. doi:10.1016/j.conbuildmat.2012.09.011

Mahakavi, P., Chithra, R., Gogoi, R., and Divyah, N. (2021). Effect of recycled aggregate and flyash on glass fiber reinforced concrete. *Mater Today Proc.* 47, 7105–7110. doi:10.1016/j.matpr.2021.06.222

Mannan, M. A., and Ganapathy, C. (2004). Concrete from an agricultural waste-oil palm shell (OPS). *Build. Environ.* 39, 441–448. doi:10.1016/j.buildenv.2003.10.007

Meraz, M. M., Mim, N. J., Mehedi, M. T., Noroozinejad Farsangi, E., Shrestha, R. K., Kader Arafin, S. A., et al. (2023). Performance evaluation of high-performance

self-compacting concrete with waste glass aggregate and metakaolin. *J. Build. Eng.* 67, 105976. doi:10.1016/j.jobe.2023.105976

Meshram, S., Raut, S. P., Ansari, K., Madurwar, M., Daniyal, M., Khan, M. A., et al. (2023). Waste slags as sustainable construction materials: a compressive review on physico mechanical properties. *J. Mater. Res. Technol.* 23, 5821–5845. doi:10.1016/j.jmrt.2023.02.176

Mim, N. J., Meraz, M. M., Islam, M. H., Noroozinejad Farsangi, E., Mehedi, M. T., Arafin, S. A. K., et al. (2023). Eco-friendly and cost-effective self-compacting concrete using waste banana leaf ash. *J. Build. Eng.* 64, 105581. doi:10.1016/j.jobe.2022.105581

Mostafa, S. A., Tayeh, B. A., and Almeshal, I. (2022). Investigation the properties of sustainable ultra-high-performance basalt fibre self-compacting concrete incorporating nano agricultural waste under normal and elevated temperatures. *Case Stud. Constr. Mater.* 17, e01453. doi:10.1016/j.cscm.2022.e01453

Nikhade, A., and Nag, A. (2022). Effective utilization of sugarcane bagasse Ash, rice husk Ash& Metakaolin in concrete. *Mater Today Proc.* 62, 3658–3664. doi:10.1016/j.matpr.2022.04.422

Nikhade, A., and Pammar, L. (2022). Parametric study of concrete by using SCBA, metakaolin, rice husk ash in concrete – a review. *Mater Today Proc.* 60, 1793–1799. doi:10.1016/j.matpr.2021.12.460

Nikhade, H., Birali, R. R. L., Ansari, K., Khan, M. A., Najm, H. M., Anas, S. M., et al. (2023). Behavior of geomaterial composite using sugar cane bagasse ash under compressive and flexural loading. *Front. Mater* 10. doi:10.3389/fmats.2023.1108717

Okamura, H., and Ouchit, M. (2018). *Self-compacting high performance concrete Development of self-compacting concrete PURPOSE OF DEVELOPMENT*.

Othuman Mydin, M. A., Jagadesh, P., Bahrami, A., Dulaimi, A., Ozkılıç, Y. O., Al Bakri Abdullah, M. M., et al. (2023). Use of calcium carbonate nanoparticles in production of nano-engineered foamed concrete. *J. Mater. Res. Technol.* 26, 4405–4422. doi:10.1016/j.jmrt.2023.08.106

Ozkılıç, Y. O., Zeybek, O., Bahrami, A., Çelik, A. I., Othuman Mydin, M. A., Karalar, M., et al. (2023). Optimum usage of waste marble powder to reduce use of cement toward eco-friendly concrete. *J. Mater. Res. Technol.* 25, 4799–4819. doi:10.1016/j.jmrt.2023.06.126

Pang, B., Zheng, H., Jin, Z., Hou, D., Zhang, Y., Song, X., et al. (2024). Inner superhydrophobic materials based on waste fly ash: microstructural morphology of microetching effects. *Compos B Eng.* 268, 111089. doi:10.1016/j.compositesb.2023.111089

Patil, A., Jayale, V., Arunachalam, K. P., Ansari, K., Avudaiappan, S., Agrawal, D., et al. (2024). Performance analysis of self-compacting concrete with use of artificial aggregate and partial replacement of cement by fly ash. *Buildings* 14, 143. doi:10.3390/buildings14010143

Poon, C. S., Kou, S. C., and Lam, L. (2006). Compressive strength, chloride diffusivity and pore structure of high performance metakaolin and silica fume concrete. *Constr. Build. Mater* 20, 858–865. doi:10.1016/j.conbuildmat.2005.07.001

Poon, C.-S., Lam, L., Kou, S. C., Wong, Y.-L., and Wong, R. (2001). Rate of pozzolanic reaction of metakaolin in high-performance cement pastes. *Cem. Concr. Res.* 31, 1301–1306. doi:10.1016/s0008-8846(01)00581-6

Prusty, J. K., Patro, S. K., and Basarkar, S. S. (2016). Concrete using agro-waste as fine aggregate for sustainable built environment – a review. *Int. J. Sustain. Built Environ.* 5, 312–333. doi:10.1016/j.ijsbe.2016.06.003

Quedou, P. G., Wirquin, E., and Bokhoree, C. (2021). Sustainable concrete: potency of sugarcane bagasse ash as a cementitious material in the construction industry. *Case Stud. Constr. Mater.* 14, e00545. doi:10.1016/j.cscm.2021.e00545

Saeed, A., Najm, H. M., Hassan, A., Sabri, M. M. S., Qaidi, S., Mashaan, N. S., et al. (2022). Properties and applications of geopolymer composites: a review study of mechanical and microstructural properties. *Materials* 15, 8250. doi:10.3390/ma15228250

Sanjeev, J., and Sai Nitesh, K. J. N. (2020). "Study on the effect of steel and glass fibers on fresh and hardened properties of vibrated concrete and self-compacting concrete," in *Mater today proc* (Elsevier Ltd), 1559–1568. doi:10.1016/j.matpr.2020.03.208

Scrivener, K. L., John, V. M., and Gartner, E. M. (2018). Eco-efficient cements: potential economically viable solutions for a low-CO2 cement-based materials industry. *Cem. Concr. Res.* 114, 2–26. doi:10.1016/j.cemconres.2018.03.015

Seelapureddy, J., Bommisetty, J., and Rao, M. V. S. (2021). "Effect of metakaolin and micro silica on strength characteristics of standard grades of self-compacting concrete," in *Mater today proc* (Elsevier Ltd), 884–890. doi:10.1016/j.matpr.2020.02.936

Setayesh Gar, P., Suresh, N., and Bindiganavile, V. (2017). Sugar cane bagasse ash as a pozzolanic admixture in concrete for resistance to sustained elevated temperatures. *Constr. Build. Mater* 153, 929–936. doi:10.1016/j.conbuildmat.2017.07.107

Shi, C., Wu, Z., Lv, K., and Wu, L. (2015). A review on mixture design methods for self-compacting concrete. *Constr. Build. Mater* 84, 387–398. doi:10.1016/j.conbuildmat.2015.03.079

Siddique, R., and Klaus, J. (2009). Influence of metakaolin on the properties of mortar and concrete: a review. *Appl. Clay Sci.* 43, 392–400. doi:10.1016/j.clay.2008.11.007

Sivakumar, V. R., Kavitha, O. R., Prince Arulraj, G., and Srisanthi, V. G. (2017). An experimental study on combined effects of glass fiber and Metakaolin on the rheological, mechanical, and durability properties of self-compacting concrete. *Appl. Clay Sci.* 147, 123–127. doi:10.1016/j.clay.2017.07.015

Sua-Iam, G., and Makul, N. (2013). Use of increasing amounts of bagasse ash waste to produce self-compacting concrete by adding limestone powder waste. *J. Clean. Prod.* 57, 308–319. doi:10.1016/j.jclepro.2013.06.009

Sun, L., Wang, C., Zhang, C., Yang, Z., Li, C., and Qiao, P. (2023). Experimental investigation on the bond performance of sea sand coral concrete with FRP bar reinforcement for marine environments. *Adv. Struct. Eng.* 26, 533–546. doi:10.1177/13694332221131153

Tang, Y., Wang, Y., Wu, D., Chen, M., Pang, L., Sun, J., et al. (2023). Exploring temperature-resilient recycled aggregate concrete with waste rubber: an experimental and multi-objective optimization analysis. *Rev. Adv. Mater. Sci.* 62. doi:10.1515/rams-2023-0347

Tibebu, A., Mekonnen, E., Kumar, L., Chimdi, J., Hailu, H., and Fikadu, N. (2022). Compression and workability behavior of chopped glass fiber reinforced concrete. *Mater Today Proc.* 62, 5087–5094. doi:10.1016/j.matpr.2022.02.427

Tu, H., Wei, Z., Bahrami, A., Ben Kahla, N., Ahmad, A., and Özkılıç, Y. O. (2023). Recent advancements and future trends in 3D concrete printing using waste materials. *Dev. Built Environ.* 16, 100187. doi:10.1016/j.dibe.2023.100187

V Bekun, F., Alola, A. A., Gyamfi, B. A., Kwakwa, P. A., and Uzuner, G. (2023). Econometrics analysis on cement production and environmental quality in European Union countries. *Int. J. Environ. Sci. Technol.* 20, 4265–4280. doi:10.1007/s13762-022-04302-9

Vivek, S. S., and Dhinakaran, G. (2017). Fresh and hardened properties of binary blend high strength self compacting concrete. *Eng. Sci. Technol. Int. J.* 20, 1173–1179. doi:10.1016/j.jestch.2017.05.003

Wagh, M., and Waghe, U. P. (2022). Development of self-compacting concrete blended with sugarcane bagasse ash. *Mater Today Proc.* 60, 1787–1792. doi:10.1016/j.matpr.2021.12.459

Wagh, M., and Waghe, U. P. (2023). *Study on fresh properties of self-compacting concrete blended with sugarcane bagasse ash, metakaolin and glass Fibre*. London: CRC Press. doi:10.1201/9781003358596

Waghe, U., Agrawal, D., Ansari, K., Wagh, M., Amran, M., Alsulami, B. T., et al. (2023). Enhancing eco-concrete performance through synergistic integration of sugarcane, metakaolin, and crumb rubber: experimental investigation and response surface optimization. *J. Eng. Res.* doi:10.1016/j.jer.2023.09.009

Wang, M., Yang, X., and Wang, W. (2022). Establishing a 3D aggregates database from X-ray CT scans of bulk concrete. *Constr. Build. Mater* 315, 125740. doi:10.1016/j.conbuildmat.2021.125740

Waqas, H. A., Bahrami, A., Sahil, M., Poshad Khan, A., Ejaz, A., Shafique, T., et al. (2023). Performance prediction of hybrid bamboo-reinforced concrete beams using gene expression programming for sustainable construction. *Materials* 16, 6788. doi:10.3390/ma16206788

Yao, X., Lyu, X., Sun, J., Wang, B., Wang, Y., Yang, M., et al. (2023). AI-based performance prediction for 3D-printed concrete considering anisotropy and steam curing condition. *Constr. Build. Mater* 375, 130898. doi:10.1016/j.conbuildmat.2023.130898

Zareei, S. A., Ameri, F., and Bahrami, N. (2018). Microstructure, strength, and durability of eco-friendly concretes containing sugarcane bagasse ash. *Constr. Build. Mater* 184, 258–268. doi:10.1016/j.conbuildmat.2018.06.153

Zeyad, A. M. (2020). Effect of fibers types on fresh properties and flexural toughness of self-compacting concrete. *J. Mater. Res. Technol.* 9, 4147–4158. doi:10.1016/j.jmrt.2020.02.042

Zhang, X., Liu, X., Zhang, S., Wang, J., Fu, L., Yang, J., et al. (2023b). Analysis on displacement-based seismic design method of recycled aggregate concrete-filled square steel tube frame structures. *Struct. Concr.* 24, 3461–3475. doi:10.1002/suco.202200720

Zhang, X., Zhou, G., Liu, X., Fan, Y., Meng, E., Yang, J., et al. (2023a). Experimental and numerical analysis of seismic behaviour for recycled aggregate concrete filled circular steel tube frames. *Comput. Concr.* 31, 537. doi:10.12989/cac.2023.31.6.537

Zhou, C., Wang, J., Shao, X., Li, L., Sun, J., and Wang, X. (2023). The feasibility of using ultra-high performance concrete (UHPC) to strengthen RC beams in torsion. *J. Mater. Res. Technol.* 24, 9961–9983. doi:10.1016/j.jmrt.2023.05.185